2019

Cross-examining Earth's oldest stromatolites: Seeing through the effects of heterogeneous deformation, metamorphism and metasomatism affecting Isua (Greenland) ~3700 Ma sedimentary rocks

Allen Phillip Nutman
University of Wollongong, anutman@uow.edu.au

Vickie C. Bennett
Australian National University (ANU), vickie.bennett@anu.edu.au

Clark R. L Friend
Gendale, UK, Chinese Academy of Geological Sciences, crlfriend@yahoo.co.uk

Martin J. Van Kranendonk
University of New South Wales, m.vankranendonk@unsw.edu.au

Leo Rothacker
leor@uow.edu.au

Publication Details

Nutman, A. P., Bennett, V. C., Friend, C. R.L., Van Kranendonk, M. J., Rothacker, L. & Chivas, A. R. (2019). Cross-examining Earth's oldest stromatolites: Seeing through the effects of heterogeneous deformation, metamorphism and metasomatism affecting Isua (Greenland) ~3700 Ma sedimentary rocks. Precambrian Research, 331 105347-1-105347-17.

See next page for additional authors

Cross-examining Earth's oldest stromatolites: Seeing through the effects of heterogeneous deformation, metamorphism and metasomatism affecting Isua (Greenland) ~3700 Ma sedimentary rocks

Abstract

The ~3700 Ma and 3800 Ma meta-volcanic and -sedimentary rocks in the Isua supracrustal belt (Greenland) were affected by heterogeneous ductile deformation under amphibolite facies conditions (~500-650 °C), and variably modified by secondary silica and carbonate mineralisation deposited from diagenetic and metasomatic fluids. Rare low-deformation areas preserve original volcanic features - submarine basaltic pillows and sedimentary features - including bedding. These are best-preserved in two dimensions on flat- to moderately-inclined outcrop surfaces, but invariably are tectonically-stretched along a steeply-plunging third dimension, through stretching in the direction of fold axes; a style of deformation found throughout Earth's history. There is a debate about whether rare relicts of ~3700 Ma stromatolites preserved in metadolomites that formed in a shallow marine setting (Nutman et al., 2016) represent bona fide biogenic primary structures fortuitously preserved in low deformation, or whether these structures are manifestations of deformation combined with non-biogenic deposition of secondary carbonate (Allwood et al., 2018). Here, we critically test the primary nature of the sedimentary rocks hosting the proposed stromatolites and also the veracity of the proposed stromatolites, by addressing the following questions: (i) Are the rocks an in situ outcrop of known age, or displaced blocks of unknown age or origin?; (ii) How much of the carbonate is of an originally sedimentary versus a secondary (i.e., metasomatic - introduced) origin?; (iii) Is the seawater-like REE + Y (rare earth element and yttrium) trace element signature carried definitely by carbonate minerals and therefore diagnostic of a cool, surficial sedimentary system?; (iv) Are the proposed stromatolites consistent with biogenicity in terms of their geometry and fine-scale layering, or could they be the product of soft sediment or structural deformation (compression in folding)? The answers to these questions, which combine diverse observations from geologic context, geochemistry and stromatolite morphology show that the weight of evidence is consistent with a biogenic origin for the stromatolites formed in a shallow water setting and are inconsistent with formation entirely through inorganic processes.

Publication Details

Nutman, A. P., Bennett, V. C., Friend, C. R.L., Van Kranendonk, M. J., Rothacker, L. & Chivas, A. R. (2019). Cross-examining Earth's oldest stromatolites: Seeing through the effects of heterogeneous deformation, metamorphism and metasomatism affecting Isua (Greenland) ~3700 Ma sedimentary rocks. Precambrian Research, 331 105347-1-105347-17.

Authors

Allen Phillip Nutman, Vickie C. Bennett, Clark R. L Friend, Martin J. Van Kranendonk, Leo Rothacker, and Allan Chivas

Cross-examining Earth's oldest stromatolites: Seeing through the effects of heterogeneous deformation, metamorphism and metasomatism affecting Isua (Greenland) ~3700 Ma sedimentary rocks

Allen P. Nutman[1,5], Vickie C. Bennett[2,5], Clark R. L. Friend[3], Martin J. Van Kranendonk[4,5,6], Leo Rothacker[1], Allan R. Chivas[1,7]

Manuscript accepted by Precambrian Research: doi.org/10.1016/j.precamres.2019.105347

[1]GeoQuEST Research Centre, School of Earth, Atmospheric and Life Sciences, University of Wollongong, Wollongong, NSW 2522, Australia

[2]Research School of Earth Sciences, Australian National University, Canberra, ACT 0200, Australia,

[3]Glendale, Tiddington, Oxon, OX9 2LQ, UK

[4]School of Biological, Earth and Environmental Sciences, University of New South Wales, Kensington, NSW 2052, Australia

[5] Australian Centre for Astrobiology, University of New South Wales, Kensington, NSW 2052 Australia

[6] Australian Research Council Centre of Excellence for Core to Crust Fluid Systems

[7] Department of Earth Sciences and Sprigg Geobiology Centre, The University of Adelaide, SA 5005, Australia

Correspondence should be directed to: Allen Nutman anutman@uow.edu.au

Abstract

The ~3700 Ma and 3800 Ma meta-volcanic and -sedimentary rocks in the Isua supracrustal belt (Greenland) were affected by heterogeneous ductile deformation under amphibolite facies conditions (~500-650°C), and variably modified by secondary silica and carbonate mineralisation deposited from diagenetic and metasomatic fluids. Rare low-deformation areas preserve original volcanic features - submarine basaltic pillows and sedimentary features - including bedding. These are best-preserved in two dimensions on flat- to moderately-inclined outcrop surfaces, but invariably are tectonically-stretched along a steeply-plunging third dimension, through stretching in the direction of fold axes; a style of deformation found throughout Earth's history.

There is a debate about whether rare relicts of ~3700 Ma stromatolites preserved in metadolomites that formed in a shallow marine setting (Nutman et al., 2016) represent *bona fide* biogenic primary structures fortuitously preserved in low deformation, or whether these structures are manifestations of deformation combined with non-biogenic deposition of secondary carbonate (Allwood et al., 2018). Here, we critically test the primary nature of the sedimentary rocks hosting the proposed stromatolites and also the veracity of the proposed stromatolites, by addressing the following questions: (i) Are the rocks an *in situ* outcrop of known age, or displaced blocks of unknown age or origin?; (ii) How much of the carbonate is of an originally sedimentary versus a secondary (i.e., metasomatic – introduced) origin?; (iii) Is the seawater-like REE+Y (rare earth element and yttrium) trace element signature carried definitely by carbonate minerals and therefore diagnostic of a cool, surficial sedimentary system?; (iv) Are the proposed stromatolites consistent with biogenicity in terms of their geometry and fine-scale layering, or could they be the product of soft sediment or structural deformation (compression in folding)? The answers to these questions, which combine diverse observations from geologic context, geochemistry and stromatolite morphology show

that the weight of evidence is consistent with a biogenic origin for the stromatolites formed in a shallow water setting and are inconsistent with formation entirely through inorganic processes.

Keywords: Isua; stromatolites; early life; dolomite; Eoarchean

1. Introduction: Dwindling signs of life in deep time

We intend that this article which tests the veracity of the oldest-proposed stromatolites should be easily accessible by a wider community of scientists outside the realms of geologists used to interpreting strongly-deformed and highly-metamorphosed ancient rocks. For this reason, included are brief explanations of terminology used in the study of deformed and metamorphosed rocks. This is particularly mindful for the astrobiology community, who are concerned with comparing and contrasting early environments on Earth and Mars.

The history of life in Earth's first billion years geological record (i.e., before ~3450 million years ago, or Ma) is controversial, with particularly debate as to the veracity of diagnostic microfossils (for example, in Greenland: Pflug and Jaescheke-Boyer, 1979, countered by Bridgwater et al., 1981 and Appel et al., 2003; in Western Australia: Schopf, 1993 and Schopf et al., 2017, countered by Brasier et al., 2002, 2005 and Bower et al., 2016). A major contributor to this controversy is the state of the preserved earliest rock record, which is vanishingly small in volume (only about one millionth of the present crust), and affected by heat (metamorphism), fluid circulation (*metasomatism – a processes causing chemical change*), and tectonic deformation (e.g., Nutman et al., 1996). Critically, high metamorphic temperatures have destroyed diagnostic biomarker molecules – the calling card of life processes – in rocks older than 1640 Ma (Brocks et al., 2005; French et al., 2015), and have made challenging the confident identification of microfossils in rocks that have largely been recrystallised (see references above). Furthermore, high-temperature deformation tends to severely limit the retention of even macroscopic primary physical features such as stromatolites in carbonate rocks, which tend to deform very easily under ductile conditions (>350°C).

However, natural systems are highly variable, and it is well known that even under extreme conditions of deformation and metamorphism, different parts of rock packages will experience marked variations in the severity of deformation, dependent largely on three factors: (a) rock properties (i.e., whether competent (strong) or incompetent (weak) at the pressure-temperature conditions under which deformation is occurring); (b) degree of fluid mobilisation/ingress to the rocks, in part controlled by primary rock properties (for example, wet mudstones metamorphose to coarsely-crystalline rocks due to their chemistry and abundance of water, whereas anhydrous quartz-rich sandstones do not coarsely recrystallise); (c) location of the rocks within a deformation regime. Significantly, it has been well-documented how the degree and style of deformation varies greatly within even a single fold structure, commonly preserving very low deformation in fold hinge regions (Ramsay and Huber, 1987).

The ~35 km long Isua supracrustal belt (ISB; Greenland), contains some tectonic slices that experienced maximum metamorphic temperatures of 550°C, and domains in which low deformation has preserved primary volcanic and sedimentary structures (e.g., Nutman et al., 1984, 2017; Appel et al., 1998; Komiya et al., 1999; Fedo, 2000). For decades, evidence for earliest life from Isua metasedimentary rocks has focussed on increasingly rigorous studies of low $^{13}C/^{12}C$ graphite from metamorphosed sedimentary protoliths, which provides compelling evidence for the presence of a biosphere near the start of Earth's rock record (Schidlowski et al., 1979; Rosing, 1999; Hassenkam et al., 2017). Additionally, other diverse lines of geochemical evidence have been postulated as signs of biogenicity, such as nitrogen abundance in micas (Stüeken, 2016) and iron isotopic ratios in banded iron formation and carbonates (Dauphas et al., 2004; Craddock and Dauphas, 2011). However, such chemical traces of life provide neither the evidence for the nature and sophistication of life 3800 to 3700 million years ago, nor of the environment it inhabited.

As more tangible evidence of life at ~3700 Ma, Nutman et al. (2016) proposed identification of stromatolites in fine- to medium-grained dolomitic (Ca-Mg carbonate) rocks from an extremely rare, low deformation area in a fold hinge (Figs. 1, 2, 3a, b). The stromatolitic metadolomitic rocks were interpreted to have been deposited in a shallow marine setting, based on geochemical data and preservation of sedimentary structures. As discussed in Nutman et al. (2016), the recognition of ~3700 Ma stromatolites is a significant step in our understanding of the history of life on Earth because stromatolites are formed by *communities* of mostly shallow water micro-organisms (see review by Riding, 2011). The Isua find therefore indicates that by 3700 Ma, close to the start of the preserved sedimentary record, life already had a significant pre-history and that a shallow marine environment is identified as a very early ecological niche, pointing to an early evolution of phototrophy is possible.

A biogenic interpretation of the Isua structures was contested recently by Allwood et al. (2018). This fosters an opportunity to examine more fully the original discovery and test the counterclaims made by these authors. Here in this paper, we present an integrated set of detailed observations combined with regional information on Isua geology that critically cross-examine the structures interpreted by Nutman et al. (2016) as stromatolites. We approach this task by posing four criteria that must be satisfactorily answered to support the biogenicity and the antiquity of the proposed stromatolites from the ISB:

(i) Geochronology and geological context: What are the age constraints; are the rocks really ~3700 Ma old? Are the proposed stromatolites an *in situ* part of the local geology, or are they exotic blocks of ambiguous age and provenance?

(ii) Quality of chemical preservation: Is the carbonate forming the stromatolites and adjacent rock layers ultimately of (recrystallised) sedimentary origin or is it secondary (i.e., metasomatic – introduced during metamorphism and deformation)?

(iii) Reliability of evidence of habitat: Is the seawater-like REE+Y (rare earth element and yttrium) trace element signature (e.g., Bau, 1999) identified by Nutman et al. (2016) from the stromatolitic-structured rocks definitely carried by carbonate minerals and therefore is diagnostic of a sedimentary/biogenic system?

(iv) Origin of rock structures and details of morphology: Do the structures described by Nutman et al. (2016) have the characteristic feature of biogenic stromatolites in terms of their geometry, or could they be the product of (a) structural deformation (i.e., folding, with/without extension), or (b) soft sediment deformation?

2. Isua: A geological overview – rocks, metamorphism, deformation, metasomatism

Although the rocks at Isua experienced the lowest metamorphic grade and locally have the best state of preservation compared with any of Earth's >3600 Ma supracrustal (i.e., *volcanic and sedimentary*) remnants, they nonetheless present significant challenges in identifying and assessing the evidence for early life. Below we provide a brief summary of the ISB and issues that must be considered when interpreting its rocks. Of particular significance concerning the stromatolite debate are the heterogeneity of deformation (amount of ductile deformation the rocks have experienced at any one locality), the degree of metamorphism and metasomatism across the ISB, and the metamorphic reactions that take place in carbonate-rich rocks under the metamorphic conditions that ISB rocks have experienced.

2.1. Geological background

The ~35 km long ISB is the world's largest preserved remnant of >3600 Ma supracrustal rocks (e.g., Allaart, 1976; Nutman et al., 1996; Nutman and Friend, 2009; Fig. 1). The ISB comprises two tectonically-juxtaposed packages of unrelated supracrustal rocks differing in age by ~100 million years, as demonstrated by compilation of precise (≤±10 Ma at 95% confidence) U-Pb zircon dating (Compston et al., 1986; Nutman et al., 1996, 1997, 2009; Crowley et al., 2002; Crowley, 2003; Nutman and Friend, 2009). Rocks in the southern and western portion of the belt are ~3800 Ma, whereas the northern and median portions of the belt are ~3700 Ma (Fig. 1; Nutman et al., 1996, 1997; Nutman and Friend, 2009, and references therein). The ~3750 Ma dividing sedimentary unit of metachert (a silica-rich sedimentary rock), banded iron formation (BIF) and dolomitic rocks lies between the ~3700 and ~3800 portions (Fig. 1; Nutman and Friend, 2009; Nutman et al., 2009). A narrow, Eoarchean meta-mylonite zone (*a folded and metamorphosed fault*) formed by ~3660 Ma, marks the northern contact of the dividing sedimentary unit with the ~3700 Ma rock package (Fig. 1). The ~3800 Ma package and the dividing sedimentary unit evolved separately from the 3700 Ma package prior to their tectonic juxtaposition before 3660 Ma - the age of the first igneous intrusions common to both terranes (Nutman et al., 1997, 2002, 2009, 2017; Crowley, 2003).

The dominant lithologies within the ~3700 and ~3800 Ma assemblages are amphibolites derived from mafic volcanic rocks of convergent plate boundary (subduction-related) geochemical affinity, metamorphosed felsic volcanic and volcaniclastic rocks, and clastic and chemical sedimentary rocks, including rare metaconglomerate, metasandstone and metadolomites, metachert and abundant metamorphosed BIF (e.g., Allaart, 1976; Dymek and Klien, 1988; Nutman et al., 1984, 2017; Komiya et al., 1999; Polat et al., 2002; Polat and Hofmann 2003, Bolhar et al., 2004, 2005; Furnes et al., 2007; Jenner et al., 2009).

The ISB is bounded by two metaplutonic (*intrusive igneous rock*) complexes (Fig. 1), with that to the south dominated by 3820-3795 Ma tonalite protoliths (K-poor granitic *sensu lato* rocks) and that to the north by 3710-3685 Ma tonalite protoliths, all of which have been cut by 3660-3640 Ma granite sheets (Nutman et al., 1996, 1997, 1999, 2000; Crowley et al., 2002; Crowley, 2003; Nutman & Friend, 2009). To the east, the ISB is obscured by the Inland Ice, and to the west it is in faulted contact with 3100-3000 Ma rocks (see Nutman and Friend, 2009 for detailed 1:20,000 scale maps of the entire belt).

2.2. Deformation history and how and where rare volcanic and sedimentary structures are preserved

Because of the ISB's complex and intense deformation history, there are only a few places where primary volcanic and sedimentary structures are preserved (e.g., Nutman et al., 1984, 2002, 2017; Appel et al., 1998; Komiya et al., 1999; Fedo, 2000). The most commonly-preserved primary structures are pillows within mafic volcanic rocks, and more rarely, bedding in BIF, in felsic volcaniclastic rocks, in conglomerates and sandstones, and in the proposed stromatolite outcrops (e.g., Nutman et al., 1984; 1997, 2016; 2017; Komiya et al., 1999; Rosing, 1999; Solvang, 1999; Fedo, 2000; Furnes et al., 2007).

Although Neoarchean (mostly at 2700-2600 Ma) tectonic deformation is low to moderate across the ISB (Bridgwater and McGregor, 1974; Nutman et al., 1984), most of the belt was strongly deformed in the Eoarchean, as demonstrated by the fact that the only weakly-deformed, still subvertical, ~3510 Ma Ameralik dykes (a suite of metamorphosed dolerite dykes) crosscut tightly-folded and strongly deformed ISB rocks (Figs. 1, 2; e.g., Bridgwater and McGregor, 1974; Nutman et al., 1984, 1996, 2002; Nutman, 1986; Myers, 2001; Hanmer and Greene, 2002).

The intensity of pre-Ameralik dyke deformation varies greatly across the limbs and hinge regions of mapped fold structures, consistent with models of finite strain identified by Ramsay and Huber (1987). The axes of most folds in the ISB are steeply plunging (typically 40-80° to south-southeast), and associated with strong stretching of rock fabrics in a direction parallel to the fold hinges (e.g., Nutman, 1986; Fig. 4). On fold limbs, this steep stretching is combined with flattening in horizontal directions, which largely destroys any primary sedimentary and volcanic features in the rocks (Fig. 4). In the hinge regions of folds, however, stretching along the fold hinge direction is accompanied by low and, in some rare cases, no deformation in the other two directions, reflecting the effect of no finite strain (at least in two dimensions) identified within hinge regions (Fig. 4: Ramsay and Huber, 1987). Thus, fold cores contain the highest possibility for the preservation of original volcanic and sedimentary structures, albeit in only two dimensions orthogonal to the stretching direction. Thus, structural geology predicts that Isua fold cores may retain primary volcanic and sedimentary textures on flat to gently-inclined outcrop surfaces, at high angles to the stretching direction. Indeed, this is exactly the observed case with both the proposed Isua stromatolites and other associated primary volcanic and sedimentary textures, which occur on flat to gently-inclined outcrop surfaces in a fold core (Fig. 2) plunging 50-60° to the southeast. This structural setting negates the concerns raised by Allwood et al. (2018) that the presence of steeply-dipping stretching fabrics at the stromatolite locality means it would be impossible for any primary sedimentary (and volcanic) textures to be preserved, and that all features on the outcrops must therefore be tectonic artefacts.

2.3. Metamorphism and Mg-Ca carbonate + silica rocks: H_2O versus CO_2 composition of intercrystalline fluids

All ISB rocks have been metamorphosed numerous times during ≥3660 to ~2500 Ma events (e.g., Baadsgaard, 1983; Boak and Dymek, 1984; Nutman et al., 1984; Nutman and

Collerson, 1991; Crowley et al. 2002). In different mylonite-bounded panels, the maximum metamorphic grade ranges from lower amphibolite (500-550°C) to middle amphibolite facies (up to 650°C) across the ISB (Boak and Dymek, 1984; Rollinson, 2003). At the stromatolite locality, the maximum metamorphic temperature is 500-550°C (the lowest in the ISB), whereas across an Eoarchean mylonite to the northwest, peak metamorphic temperatures were ≥600°C (Fig. 1; Boak and Dymek, 1984; Rollinson, 2003). The parts of the ISB with different maximum metamorphic temperatures are all cut by the ~3510 Ma Ameralik dykes. These dykes all show uniform, probably Neoarchean (Nutman, 1986; Rollinson, 2003) epidote amphibolite facies metamorphism (500-550°C), attesting to the polymetamorphic history of the ISB.

Experiments of reactions in mixed quartz + dolomite rocks (which represent the main minerals of the Nutman et al. (2016) proposed stromatolite-bearing rocks) were summarised by Skippen (1974) and are reproduced here in Figure 5. This shows that at 500-550°C, quartz + dolomite will still be stable if the intercrystalline fluid phase (films of fluid along the mineral grain boundaries of the rock) is CO_2-rich (XCO_2 approaching 1). In contrast, these minerals would react in the presence of a more H_2O-rich fluid (decreased XCO_2) to form the silicate minerals talc or tremolite (crossing the reaction line to the *tr+cc* field on Fig. 5). One of these reactions is as follows:

5dolomite + 8quartz + 1H_2O ↔ 1Mg-Ca tremolite (H_2O-bearing silicate) +3calcite +7CO_2

This classic experimental metamorphic petrology (Fig. 5) shows how changes in XCO_2 versus XH_2O in the rock's intercrystalline fluid phase can, at *constant temperature and confining pressure*, drive a reaction from the carbonate + quartz side to the tremolite side (green arrow on Fig. 5), or *vice versa*. Thus, under conditions that drive the above reaction from the *left to the right*, either 'excess' quartz or dolomite will coexist with tremolite on completion of the reaction, depending on the relative original amounts of quartz versus dolomite. This demonstrates that the details in metamorphic reactions related to the composition of the intercrystalline fluid phase are of crucial importance in understanding the variable appearance of the rocks around the stromatolite locality, and how it is possible for fine-grained original sedimentary structures in quartz + dolomite to be preserved *very locally* within an otherwise highly recrystallised coarse-grained tremolite-bearing marble (the metamorphic equivalent of pre-metamorphic dolomite+quartz: Nutman et al., 2016). Mapping of the fold structure in which the stromatolites were discovered shows the preservation of sedimentary cross-bedding in addition to the stromatolite structures is only in small domains where the stability between quartz and dolomite has been preserved. These are flanked by domains where quartz and dolomite have reacted to form coarse-grained tremolite (Fig. 2).

2.4. Microtextures of Isua carbonate rocks

All ISB rocks have been metamorphosed, and consist of mosaics of minerals that formed during one or more high temperature events. Thus, an ISB amphibolite that now consists of a mosaic of fine-grained metamorphic (~550°C) hornblende + plagioclase + quartz + epidote, but retains relict pillow structures can be safely inferred to have originated from a cryptocrystalline to fine-grained basalt, with an original assemblage of volcanic glass with small plagioclase + clinopyroxene phenocrysts. Similarly, Isua metadolomitic sedimentary rocks with/without stromatolites and cross-bedded quartz-rich sandstone interbeds that now consist of medium-grained granoblastic (sugar-like texture) mosaics of dolomite ± quartz ± mica (Fig. 6a), can equally safely be inferred to originate from a mixture of sedimentary carbonate + quartz + small amounts of clay (mud). An example of ancient stromatolitic dolomites where this reasoning has been applied is with the ~3430-3350 Ma stromatolites of the Strelley Pool Formation (Pilbara, Australia), where metamorphic recrystallisation under much lower temperatures (<300°C) have produced granoblastic dolomite grain textures in some rocks still identified as stromatolites. All these stromatolites of the Strelley Pool Formation are still accepted as biogenic, even where recrystallisation has destroyed fine layering (Hofmann et al., 1999; Allwood et al., 2006).

2.5. Metasomatism: Introduction of secondary carbonate and silica into volcanic and sedimentary rocks

Regardless of age, metamorphism and deformation of volcanic and sedimentary rocks commonly results in the introduction of secondary carbonate and quartz, deposited in fissures and/or penetratively through the rock. These are precipitated from hot fluids rich in dissolved mineral components. It has long been recognised that secondary carbonate +/- quartz mineralisation occurs in Isua (e.g., Nutman et al., 1984), generating debate as to whether *all* Isua carbonate is of secondary origin and unrelated to sedimentary processes (e.g., Rose et al. 1996; Rosing et al., 1996), or whether some carbonates contain original (metamorphosed) sedimentary carbonate with/without secondary carbonate veins and patches (e.g., Allaart, 1976; Nutman et al., 1984, 2010, 2017; Bohlar et al., 2005; Friend et al., 2007).

The discrimination between metamorphosed original carbonate-bearing sedimentary rock units and carbonates formed by later post-depositional events can be made by broad field examination, together with geochemical (REE + Y, and carbon isotope) analyses (e.g., Van Kranendonk et al., 2003). It is important to note that field relationships can vary, even on individual outcrops, meaning that careful observation must be made of the relationship between units along and across strike (strike is the trend of layering in the rocks). In the Discussion section below, the importance of this is highlighted by a comparative case study of the northeastern end of the proposed stromatolite site ‘A’ studied by Nutman et al. (2016), versus the southwestern end of the same ~4 m long outcrop studied by Allwood et al. (2018).

3. Testable hypotheses for the proposed 3700 Ma Isua stromatolites

3.1a. Are the host rocks an intact part of Isua's well-dated stratigraphy or are they dislocated blocks, e.g. glacial erratics of unknown age and provenance?

Parts of the ISB are poorly exposed due to an extensive blanket of glacial moraine, left by retreat of the icesheet. Erratics in this moraine, transported for tens or more of kilometres, can be of considerable size – up to tens of metres across. Thus, care must always be exercised that rocks of special scientific interest are a contiguous part of the outcrop, and not exotic blocks that were carried from afar by ice. Although most erratic material at Isua consists of locally-sourced metamorphosed and deformed Archean lithologies, A. Nutman and C.R.L. Friend have found rare erratics of seemingly non-metamorphosed sedimentary rocks both at Isua and at the same latitude in the Ammassalik area on Greenland's east coast (unpublished field observations). This suggests that there is a source of younger, non-metamorphosed sedimentary rocks under the icecap, probably as cover to the Archean basement. Therefore, it is necessary to ensure that the proposed Isua stromatolites and associated sedimentary rocks (Nutman et al., 2016) are genuinely part of Isua's Eoarchean geology, and are not unrelated exotic (younger?) material.

Any erratic block transported from afar would have structural and compositional features mis-matched with respect to the adjacent bedrock geology. As shown in Figure 7, the Nutman et al. (2016) stromatolite site 'A' is demonstrably an *in situ* outcrop, because it occurs within 20 cm of a compositionally identical bedrock outcrop whose layering is of the same orientation to that within the stromatolite discovery outcrop. A similar situation can be demonstrated for the stromatolite site B outcrop (Extended Data Fig. 2D in Nutman et al., 2016). Furthermore, as noted by Allwood et al. (2018), the stromatolite structures have been affected by tectonic stretching, as are surrounding rocks, and they contain a metamorphic assemblage that is consistent with the regional metamorphic grade (Nutman et al., 2016).

Therefore, the first criterion is satisfied; the rocks that contain the proposed stromatolites are part of Isua's bedrock geology.

3.1b Confirmation of an Eoarchean age

The ISB is a tectonic assemblage of a ~3800 Ma southern terrane and a ~3700 Ma northern terrane, tectonically juxtaposed against each other by 3660 Ma (Nutman et al., 1997, 2002, 2009). Given that the ISB is already known to be composite in age, the possibility needs to be entertained that the stromatolite-bearing unit is an invagination or tectonic sliver of a younger, post-3700 Ma, assemblage. Such a scenario is found in the Nuvvuagittuq supracrustal rocks of Canada, where the Eoarchean lithologies contain an often-ignored sliver of metasedimentary rocks with detrital zircons as young as 3370 Ma (Darling et al., 2013). For Isua, there are two strong lines of evidence that counter against the proposed stromatolites being much younger. First, the tight fold containing the stromatolite-bearing unit is cut discordantly by a swarm of amphibolitised, variably deformed, metadolerite dykes (Figs. 1, 2), from which a nearby member has yielded a magmatic (high Th/U) zircon U-Pb age of 3511±18 Ma (Nutman and Friend, 2009) providing an absolute minimum age constraint. Second, more deformed and recrystallised quartz + tremolite ± carbonate rocks that are the <100 m distant lateral equivalents of the proposed stromatolite occurrences have yielded sparse volcanogenic or detrital zircons with ages of 3740-3700 Ma, a BIF unit that is stratigraphically and structurally above the proposed stromatolite bearing-lithologies yield sparse ~3695 Ma volcanogenic zircons and andesitic volcanic rocks that stratigraphically underlie them have a zircon age of 3709±9 Ma (Figs. 1, 2; Nutman et al., 2002, 2009; Nutman and Friend, 2009). Collectively, these results indicate that the proposed stromatolite-bearing lithologies must be ~3700 Ma old.

3.2. Primary sedimentary versus secondary metamorphic/metasomatic origin of carbonate?

Is the stromatolite dolomitic (Mg-Ca) carbonate ultimately of sedimentary (but recrystallised) origin, or did it originate entirely from secondary metamorphic/metasomatic deposits? If the latter, did the carbonate form by the introduction of CO_2-rich fluids to cause reactions that deposited carbonate in originally silicate-only rocks?

The fine-scale quartz and dolomite layering of the proposed stromatolite-bearing metadolomite at site ‘A’ is at the edge of a large outcrop, over which it is progressively overprinted by coarse-grained tremolite in rocks that retain only a crude semblance of the original fine-scale layering, interpreted as bedding. Figure 8a demonstrates this ~5m from the stromatolite ‘A’ site where a ~1 m wide residual kernel with fine-scale dolomite + quartz bedding is surrounded by amphibole-rich rocks. This clearly shows that the tremolite growth was caused by ingress of higher XH_2O fluid across the bedding within a precursor fine-grained dolomite + quartz rock. If one considers the alternative reaction, it is actually *impossible* to form a fine-grained, delicately-layered quartz + dolomite rock by adding CO_2 to a coarse-grained amphibole-rich rock. This same observation is shown in a less dramatic way on the ‘stromatolite’ outcrops themselves. For example, at the proposed stromatolite ‘B’ site of Nutman et al. (2016), thin amphibole-rich veins (formed by the introduction of water) cut across a fine-grained dolomite + quartz matrix, proving the older age for the carbonate + quartz.

Thus, mineral textures and metamorphic reaction evidence integrated with field mapping shows that the fine-grained quartz + dolomite assemblages are relicts of an early assemblage (Figs. 2, 8a), and were *not* formed by carbonic metasomatism of Si-rich rocks. However, it should be stressed that throughout the ISB there is widespread development of secondary carbonate veins, emplaced during the belt’s multistage Archean tectonothermal history (e.g., Nutman et al., 1984, 2010; Rose et al., 1986; Rosing et al., 1996). Many such veins can be recognised and distinguished in the field by their coarse grainsize, discordance to layering in host rocks (Fig. 3c, d and Fig. 8b), and, in some examples, reaction selvedges of tremolite, talc or diopside. The geochemistry of such vein materials are discussed separately, below.

3.4. Carbonate chemistry

Importantly, sedimentary carbonate is compositionally distinct, composed of dolomite (Ca-Mg) and/or calcite (or, in Recent rocks, aragonite and/or high-Mg calcite). In contrast, as discussed more fully below, carbonate that is of metamorphic or metasomatic origin is well known to be iron-rich (ankerite, siderite) and to have distinctive geochemical properties.

Low temperature dolomite deposited in sedimentary settings in the oceans and in pore waters near Earth's surface forms almost exclusively through biomediation, as determined by field observations and laboratory experiments (e.g., Vasconcelos et al., 1995; Roberts et al., 2004; Wright and Oren, 2005; Wright and Wacey, 2005). Marine dolomites also carry a characteristic seawater-like rare earth element (REE) + yttrium (Y), normalised to PAAS (post-Archean average shale) normalised signature (Bau and Dulski, 1996; Bau, 1999); a feature recognised for the Isua stromatolitic metadolomites (Nutman et al., 2016). For a marine origin of the carbonates to be inferred, it is important that the seawater signature is derived from demonstrably marine precipitates and not any foreign material, including landmass-derived mud that may be incorporated with the carbonates. For example, if the REE+Y seawater signature was *not* carried by the dolomite, this could place doubts on the Nutman et al. (2016) proposed formation of the protolith carbonate from seawater.

In the Isua stromatolitic metadolomites, as with other ancient to modern metacarbonates (e.g., Van Kranendonk et al., 2003), the seawater-like REE+Y signature comprises: positive La anomalies relative to Pr; the strong relative depletion of the light REE

(LREE) over the heavy REE (HREE); a strongly super-chondritic Y/Ho ratio, expressed as a positive Y anomaly in the pattern; and positive Eu anomalies (Bau, 1999). These features are well demonstrated to represent unique complexation phenomena in the active hydrological cycle (e.g., Bau, 1999; Kamber et al., 2014) and differ from the REE+Y patterns seen in the vast majority of other geological materials, thus providing a diagnostic signature of precipitation from low temperature, typically marine, waters (e.g., Bau and Dulski, 1996; Bau, 1999; Van Kranendonk et al., 2003; Kamber et al., 2014).

The specific mineralogy of the proposed Isua stromatolitic metadolomite beds is ferroan dolomite ± quartz ± Mg-rich biotite (Nutman et al., 2016). Excluding the quartz, which is essentially devoid of REE+Y, the REE+Y budget of the rock will thus be distributed between the carbonate and the biotite (a silicate mineral). The REE+Y signature has been assessed previously by bulk analyses of ~200 g powder aliquots of whole rock samples (Friend et al., 2007; Nutman et al., 2016), and via LA-ICP-MS transects over site 'A' dolomite grain aggregates in the proposed stromatolites and bounding layers (Table 1; Fig. 9; Nutman et al., 2016). In both instances, a seawater-like REE+Y signature was revealed, and on mass-balance considerations, would suggest these elements are predominantly lodged in the abundant ferroan dolomite.

In order to confirm the presence of the seawater signature within the ferroan dolomite, we analysed individual carbonate grains from within the proposed stromatolites by spot LA-ICP-MS (Fig. 9, Table 1). The analytical methods and data normalisation are presented in the Appendix. Pure dolomite spot analyses in site 'A' and 'B' proposed stromatolites and in adjacent bedded, but non-stromatolitic metadolomites (the latter reported in Nutman et al., 2016) all display the characteristic seawater-like REE+Y signatures (Fig. 9). These results contrast with samples that contain a higher proportion of protolith silicate minerals (Mg-biotite, originating from mud, demonstrated in the analyses by higher K, Ti) display a less pure seawater-like signature (labelled '*A dirty*' in Table 1) with an increase in the LREE that reduces the Yb/La ratio and the La, Ce and Y positive anomalies (Fig. 9: Nutman et al., 2016). This is in accordance with all studies of 'contaminated' carbonate sedimentary rocks throughout Earth history (e.g., Kamber et al., 2014).

This evidence negates the claim of Allwood et al. (2018) that the seawater-like signature resides in the micaceous (muddy) component, rather than the carbonate. As noted by Allwood et al. (2010) for recrystallised stromatolitic metadolomites from the Pilbara that contain REE+Y seawater-like signatures identical to the Isua carbonates discussed here: "*These REE characteristics are extremely unlikely to have been produced by circulation of seawater through originally non-marine sediments, and fortuitous reproduction of the seawater REE anomalies by original precipitation from fluids of a completely non-marine origin is equally improbable as those characteristics form by complex and unique natural processes (e.g. Bau, 1999)*".

Importantly, cross-cutting secondary vein carbonates (ankerite, or siderite) from Isua, which are distinct in the field (Fig. 8b) from the stromatolite-bearing carbonates, have variable REE+Y signatures that differ completely to dolomite derived through original precipitation from seawater. This difference in REE+Y geochemistry is demonstrated by a secondary carbonate vein ~25 m from the site 'A' stromatolite (Figs. 8b, 9; Table 1).

In some cases, carbonates that were originally deposited from seawater may become remobilised and injected into veins in other lithologies during diagenesis (*the low temperature processes whereby an unconsolidated sediment is converted into a sedimentary rock*) or metamorphism. Indeed, remobilisation of carbonate (dissolution and reprecipitation) is a very widespread occurrence in the diagenesis of carbonate sedimentary rocks. In the absence of a new introduced fluid component, remobilised marine carbonates will retain their original seawater-like REE+Y signature as noted, for example, for recrystallised Strelley Pool

Formation stromatolitic dolomites of the Pilbara Craton (Van Kranendonk et al., 2003; Allwood et al., 2010).

3.4 . Do the proposed stromatolites require biogenic interaction or are they tectonic or sedimentalogical artefacts?

Soft sediment deformation features

One suggested origin of the proposed Isua stromatolite structures is as sedimentary flame structures (D. Flannery, pers. comm., 2018), which can result when a heavy, thick, and commonly coarse-grained bed of clastic sediment (e.g., sand, or gravel) is instantaneously deposited on a bed of finer-grained, and still wet, fine-grained clastic sediment (e.g., mud or silt). The resultant density loading causes sinking of the heavier material down into the finer-grained underlying material, and injection of that soft, wet underlying material as “flames” up into the base of the coarser-grained load. This produces a set of features consisting of commonly (but not always) evenly spaced, upward-pointing, commonly asymmetrical narrow flames on either side of broad, downward-curved lobes of a single contact interface between the two materials. The overlying, denser bed is generally much thicker than the underlying, finer-grained bed, but the lower bed must have some thickness (typically > 2 cm) in order to feed material into the flames. Both the overlying and underlying contacts of adjacent beds may be flat and unaffected by the gravitationally-driven exchange of material between the two affected beds. In some examples, faint traces of bedding in the overlying coarser sediment are deflected upwards at the flanks of the flame structures, whereas the flames themselves commonly do not show curved internal bedding traces and may be characterised by extremely thin, commonly wispy, tips. Typically, the height of flame structures is much less than the thickness of the overlying bed that caused them to form.

As with clastic sedimentary sequences that contain flame structures, the Isua stromatolites occur within a compositionally layered succession, consisting of interbedded units of chemical sedimentary rock (stromatolitic dolomite) and micaceous calc-silicates, which were originally fine-grained clay-bearing carbonate silts or muds with a crustally-sourced mud component.

As noted by Nutman et al. (2016), the Isua stromatolitic beds are compositionally distinct from overlying and underlying beds in being relatively pure dolomite+quartz, with little or no mud component. The Isua stromatolites differ from sedimentary flame structures because: 1) they are tall structures relative to the thickness of the source bed; 2) they contain relicts of internal lamination that reach right up into the peak of the stromatolites; 3) the overlying sediment onlaps the stromatolites and does not deflect upwards towards the edges of the flames; 4) there are no wispy tips to the stromatolites, which rather have rather broad, domed tops. Thus an origin of the stromatolites as flame structures can be ruled out.

<u>Tectonic folds</u>

The outcrops present 2D cross-sections through the steeply-dipping beds with proposed stromatolite structures (Fig. 3). The primary bedding of the outcrops is no longer in its original horizontal orientation because of folding (Figs. 2 and 4). This precludes the outcrop surfaces following deposition/bedding surfaces, on which the coniform-domical 3D morphology of stromatolites is most readily seen (e.g., Riding, 2011). Rather, the Isua outcrops are orientated as oblique 'cross-sections' through the bedded surfaces, providing optimal views of the best-preserved pre-folding geometric relationships on these surfaces, and as explained above (Figs. 3 and 4), this is *perpendicular* to the stretching direction (plunging 50-60° to southeast). In contrast, along the plunging stretching direction, any primary features will be drawn-out and disrupted. This relationship is clearly shown, albeit misinterpreted, in Extended Data Figure 3 of Allwood et al. (2018).

For the Isua proposed stromatolites to represent folds, their crests should be elongated in the direction of the fold axis and stretching direction. Alternatively, if the stromatolites are *bona fide* coniform structures, their crests will form cones that may be elongated along the stretching direction. As shown in Figure 10a and via a manipulable 3D pdf of this example [the *42 Mb 3D pdf file will be linked here*], cuts of a site 'A' proposed stromatolite in all directions parallel, and perpendicular, to the stretching direction demonstrates a coniform top in all three directions, and thus a non-fold geometry.

Another important feature relating to a possible fold origin is the relationship between the bottom and top contacts of the proposed stromatolite structures and compositional layering in the surrounding sedimentary rocks. This is because stromatolites are biogenic constructs that grow up from a generating surface to keep above the level of clastic material accumulating around them (Riding, 2011). This will lead to the stromatolites initiating from a flat substrate (originally a tabular microbial mat) and growing upwards into a variety of shapes (domes, clubs, columns, cones) as the sediment accumulates (Riding, 2011). This will give rise to a strong asymmetry between the bounding bottom and top surfaces of a stromatolite horizon, and also result in onlap of the sediment layers onto the stromatolite margins as the sediment accumulates against the sides of the positive growth structures of the stromatolites (e.g., Van Kranendonk, 2011). As noted by Nutman et al. (2016) as a key feature supporting biogenicity, Figure 10a demonstrates this feature for the site 'A' proposed stromatolites, with the onlapping layering denoted by coloured lines. Figure 10b denotes the onlapping of layering on the smaller amplitude site 'B' stromatolites, via a thin section image. Some of these laminations are inclined relative to underlying upper surface of the stromatolite by up to an apparent dip of ~30°, significantly greater than the angle of repose for loose sediment, indicative of microbial binding (e.g., Van Kranendonk et al., 2003).

Allwood et al. (2018) suggested that the observed compositional layering onlapping sedimentary bedding in the Isua stromatolites could instead be vestiges of an earlier tectonic fabric. But tectonic foliations are planar alignments of mineral grains, not bedding-like layer structures. And even if this were the case, then such a fabric should pass into the stromatolite structures, but it does not (Figs. 3a and 10a, and noted also by Allwood et al., 2018). Despite the recrystallisation and coarsenin of grain size during metamorphism, vestiges of layering are also revealed by mapping techniques, such as brightness in SEM backscattered imaging (Nutman et al., 2016; Fig. 10c). Furthermore, the compositional layering adjacent to the proposed stromatolites display truncation and variation from planar to curvilinear, as is most clearly demonstrated at site 'B' (Fig. 11a) and by nearby cross bedding in quartz + dolomite sandstones (site 'D' on Fig. 2 and Fig. 11b). Such geometric relations cannot be formed by deformation. Instead, in the sandstones they are consistent with an interpretation as swalely cross bedding and scouring, types of clastic sedimentary structures observed in variable-energy shallow marine settings. Therefore, within, and only within, the area immediately around the proposed stromatolite occurrences, the earliest compositional layering has all the attributes of sedimentary bedding, and in no way resembles tectonic fabrics. Therefore these rocks, in extremely rare locations in the hinge regions of the fold (Fig. 2), are preserving sedimentary structures on the mm- to cm-scale. However, given that these sedimentary bedding forms are developed in detrital rocks, why then is not the clastic grain texture not visible in the thin section scale? This is because of recrystallisation during the superimposed 500-550°C metamorphism moved grain boundaries to give a secondary granoblastic texture (e.g., Fig. 6a), marked by straight grain boundaries and often ~120° grain junctions.

By way of contrast, Nutman et al. (2016) noted a penetrative tectonic foliation at a high angle to what they interpreted as bedding. These fabrics are also present in the Allwood et al. (2018) study, in the same orientation. Critically, these fabrics are oriented along the direction of the axial plane of the fold that affects the stromatolitic bedding and thus is consistent with the identified structural history of the locality. Such is not the case for the compositional layering of the stromatolite-bearing outcrops, which is clearly affected by, and thus pre-dates, the large-scale folding.

Deformation intensity and folding

In the best-preserved examples of the proposed stromatolites, Nutman et al. (2016) showed that the deformation giving a weak cross-cutting foliation cannot account for the structures identified as stromatolites. This is because the compression recorded by the rocks only produces micro-scale folds (mm-scale crenulations) of mm-scale bedding layers, which contrast dramatically with the centimetre-scale amplitude along only one (the uppermost) side of the proposed stromatolites (Figs. 3a, b). Also clearly visible (e.g., the layer marked with a horizontal white arrow of Fig. 3b) is that the mm-scale microfolds of compositional layers are symmetrical (i.e. up and down, with repeatable wavelength) and affect both the upper and lower contacts of each of the folded layers. This contrast dramatically with the sharp-sided, asymmetrical geometry of proposed stromatolites, which are up to 3 cm high coniform shapes, *with flat bases*. Critically this identical geometry applies to several structures all along the same bedding plane, as well as to several beds of these structures within the one outcrop. Compressional deformation cannot produce such features. The weak folding recorded by the mm-scale microfolds matches the mild nature of the deformation as indicated by the weak transecting micaceous foliation (blue lines on Fig. 3b), which shows that the compression in this part of the outcrop was very mild indeed. Furthermore, compression (i) *cannot* produce folds that have flat bases and sharply-peaked tops, and (ii) instead would produce individual layers (beds) that would be curved (folded) across the full 4 m extent of site 'A' outcrop, rather than the flat geometry, as found. This repudiates the claim of Allwood et al. (2018) that the proposed stromatolites of Nutman et al. (2016) are simply corrugations formed in the core of a fold. The same cannot be said for the structures studied by Allwood et al. (2018), which are starting to show folded basal and upper contacts indicative of an incremental higher degree of deformation on parts of the outcrops with less favourable preservation of sedimentary structures (their Figure 2c). For this reason, we avoided analysis of these structures at that end of the outcrop when we discovered it.

Critical in this example is the fact that the pale, more micaceous, bed that immediately overlies the sharply peaked, dolomite-rich proposed stromatolites shows a flat upper contact unaffected by folding. This is dramatic evidence of the onlap nature of the sedimentary units (defined by changes in composition) that overlie the stromatolites, and it absolutely disproves folding as the origin of the stromatolites. If folding were the cause of the stromatolites, then the paler bed would also be folded.

Recrystallisation of layering

All ancient stromatolites are recrystallised, including even the best-preserved material described for publications (as with the Isua proposed stromatolites of Nutman et al. 2016). Yet even the 'best' examples have layering that has been corrupted to a certain degree. For example, the well-preserved ~2720 Ma stromatolites from the Tumbiana Formation (e.g., Figure 13f of Flannery et al., 2016) clearly show the effects of silicification that has partially destroyed the finer-scale layering present in the primary dolomite. Indeed, degradation of primary lamination in stromatolites commences during microbial reworking of organic and carbonate matter, even as the structures are forming (e.g., Reid et al., 2000). Therefore, the imperfectly-preserved internal lamination in the Isua proposed stromatolites (Nutman et al., 2016, and see Figures 3a, b here) does not negate that the described features are stromatolites. This is particularly the case when account is taken of the degree to which lamination is destroyed in younger stromatolites with a less severe deformational and metamorphic overprint (for example Pilbara stromatolites, as illustrated in Fig. 6b).

4. Discussion

4.1. Two studies of Isua stromatolite site 'A'

Two studies have been undertaken on the site 'A' outcrop – Nutman et al. (2016), focussing on the lower deformation northeastern end, and Allwood et al. (2018) less than 4 metres away on its southwestern end, in a more highly deformed and altered part of it. These authors give diametrically opposing interpretations; with the former concluding there is primary (albeit recrystallised) sedimentary bedding and stromatolites that have been only mildly modified by superimposed deformation and metamorphism, whereas the latter proposing that *all* features are the product of secondary chemical alteration processes and deformation. Here, we provide a detailed examination of this outcrop to demonstrate that these differences have arisen because this is a case of *comparing apples with oranges*, as a result of significant variation in the degree of deformation and secondary chemical alteration across the ~4 m long outcrop.

Specifically, the southwestern end of the site 'A' outcrop has been affected by increasing superimposed deformation and secondary carbonate veining, which has caused more complicated geometric relationships. Here, we contend that these complicating overprinting factors are the cause of what Allwood et al. (2018) interpreted as a structure that superficially resembles an "upside down" facing stromatolite (labelled 'A' on Fig. 3c). The potential stromatolite-bearing horizon (S) in this photograph, together with underlying layers labelled B, and C, are clearly cut by an interfingering, but largely bedding-parallel vein of secondary, dark brown carbonate (shown by red arrows on Figs. 3c, d). This secondary carbonate occurs throughout Isua and is readily recognised by its dark brown colour as most likely being ankerite, a Fe-rich carbonate that weathers in this this very specific way. Critically, secondary carbonate veins are absent from the outcrop parts studied by Nutman et al. (2016), in which the stromatolites are composed of dolomite, a carbonate mineral known associated with stromatolites throughout the geological record. We interpret the apparent “upside-down” feature identified by Allwood et al. (2018; ‘A’ in Fig. 3c) as a remnant of an original bed, underlying the stromatolite horizon, which has been transected by splays of the secondary carbonate vein, creating a downward-tapering wedge-shaped remnant of the original bed. Importantly, faint traces of layering in bed A are horizontal in the “upside-down” feature, as in other parts of underlying beds A, B and C. This horizontal layering contrasts with the traces of faint layering in the well-preserved stromatolites described by Nutman et al. (2016), which is convex, and subparallel to their upper contact. Importantly, the secondary carbonate vein network also cuts up through parts of upward-pointing (what we would regard as biogenic) stromatolites (the red arrows marked ‘*’ in Figs. 3c, d), in the Allwood et al. (2018) part of the outcrop, clearly demonstrating the secondary nature of these veins.

4.2. Carbon isotope signatures

The Isua proposed dolomitic stromatolites and interbedded muddy metadolomites contain positive $\delta^{13}C$ values (~+1‰) that are significantly distinct from other Isua carbonates of metamorphic, or uncertain origin (Fig. 12). A compilation of carbon isotopic data, which is mostly from rocks with extensive calc-silicate (e.g., tremolite) development and that includes secondary carbonate veins, $\delta^{13}C_{VPDB}$ values typically lie in the range 0 to -7‰, well below that of the stromatolitic carbonate, which clusters tightly at about $\delta^{13}C_{VPDB} \approx +1‰$. This uniform positive value is significant, as it is within the narrow range common for marine carbonates throughout the entire geological record (Veizer and Hoefs, 1976; Schidlowski, 2001).

4.3. The case for biogenicity of Isua stromatolites

There have been several previous studies that have proposed criteria that serve to illustrate whether stromatolite structures might be biologically produced. These criteria have been controversial since they were first made by Kalkowsky (1908), which stated that the organic portion should not be fossilised (see, Krumbein, 1983). The criteria were further modified by Walter (1976), and Buick et al. (1981), who posed several questions to establish whether a stromatolite structure might be biological or not. These are:

(1) The structures must occur in undoubted sedimentary or metasedimentary rocks. *The Isua rocks are shown to be sedimentary through their structures and seawater-like geochemical signatures.*

(2) It must be demonstrated that the structures are synsedimentary (formed at the same time the sediments constituting the bed were being deposited). *The Isua conical/domical structures can be shown to be syn-sedimentary via onlap relationships of overlying slightly muddy metadolomites*.

(3) There should be a preponderance of convex-upward structures. *The preserved Isua examples are convex-upward, even conical structures*.

(4) Laminae should thicken over crests of flexures. *Despite metamorphism to amphibolite facies with stretching deformation in one dimension, there is still some evidence that sedimentary laminae change thickness (Fig. 3b).*

(5) Laminations should be wavy, wrinkled, and/or have several orders of curvature. *Due to subsequent metamorphism and deformation the nature of the laminae in the Isua material has been modified, as it has in even younger metadolomites of the Strelly Pool Formation, in which a biogenic origin is not contested*.

(6) Microfossils should be present in the structures. It is accepted that this is frequently the case, yet a biological origin is still regarded as most likely (see Awramik and Grey, 2005).

Like the vast majority of fossil stromatolites across the geological record, no microfossils have been identified in the Isua stromatolites.

(7) Changes in composition of microfossil assemblages should be accompanied by morphological changes of the stromatolite. *Not found, and barely found in any age*.

(8) Microfossils must be organized in a manner indicating trapping, binding or precipitation of sediment by the organisms. *No microfossils, but the domal morphology of the Isua stromatolites is consistent with trapping and binding of sediment*.

Krumbein (1983) also looked at both fossil and modern extant stromatolites and set out a basic set of 10 criteria regarding whether a structure was a (biogenic) stromatolite or not. Some of these criteria, such as "*Stromatolites are alternatingly or evenly laminated consolidated rocks*" can be applied relatively easily, whilst "*Their lamination is related to the activity of micro-organisms*" is much more difficult to apply to many fossil examples. Krumbein (1983) then proposed a new definition derived from as wide a data-base as possible. Most of the requirements of this definition are passed by the Isua structures but, like those of the Pilbara, there is not the absolute proof that organisms were involved, as their remains are not preserved. These are exacting criteria and there are few stromatolites from the geological record that would unambiguously meet *all* the criteria. Grotzinger and Knoll (1999) emphasise that many ancient stromatolites are recrystallised which leads to modification of the laminae and in the worst cases leaves a crude layering of silt and clay along the altered surfaces. In the Isua case, the laminae can be seen in varying states of destruction progressively away from the core of the regional fold (Fig. 2a), where the best examples are preserved.

It is generally agreed that there is no single criteria that can unequivocally prove a biogenic origin. However, there is an emerging consensus that strong cases for biogenicity in Archean stromatolites can be constructed by careful integration of geological context, morphology and geochemistry, using data from a variety of observational and analytical approaches (e.g., Awramik and Grey, 2005; Van Kranendonk, 2011).

Strict criteria for biogenic Archean stromatolites include the identification of microfossils and demonstration that microbes participated in the carbonate precipitation. However, this requires exceptional preservation, such that the oldest stromatolites that perhaps fulfil these criteria being drill core samples from the 2700 Ma Tumbiana Formation, Australia (Lepot et al, 2008). Because microfossils are exceedingly rare in stromatolites of all ages, adherence to this criterion would mean dismissing the potential biogenicity of the vast majority of occurrences that have exquisite morphological expression. It is noteworthy that formerly contentious stromatolite localities including the well-preserved ~3400 Ma Strelley Pool Formation and the 3480 Ma Dresser Formation are now widely accepted as having a biogenic origin, despite the absence of microfossil preservation (e.g., Allwood et al., 2006; Van Kranendonk, 2006, 2011). Going back to >3500 Ma, much more limited outcrop and higher metamorphic temperatures and degrees of deformation and recrystallisation presents a greater set of challenges for identification of early life. Yet, it is this period of Earth's history that can best tell us about life's origins and early habitats and may provide best planetary analogues.

We have extended the approach that has been developed for recognising biogenicity of 2700 to 3500 Ma stromatolites back to the Isua 3700 Ma stromatolites. Importantly, this approach continues to be validated by a range of complementary discoveries including microfossils in associated Palaeoarchean cherts (Alleon et al, 2018). Thus, by careful appraisal of a range of evidence including geochemical features and detailed consideration of stromatolite morphology in the context of the deformation and metamorphic state of the outcrops, we propose that the structures and mineralogy described by Nutman et al. (2016) fit the interpretation of a currently unique example of Eoarchean stromatolites. Given the weight of evidence based on diverse range of analytical, morphologic and geological observations, the Isua stromatolites must be considered with a high probability as biogenic features attesting to the presence of life at 3.7 Ga. This is in accord with integrated genomic and fossil evidence requiring origin of life >3900 Ma (Betts et al., 2018) and complementary isotopic evidence (e.g., Rosing, 1999; Hassenkam et al, 2017) supporting life in the Isua rocks at 3700 Ma. However even these “best of the best” early Archean samples highlight the challenges of extending knowledge of life nature and environments to the start of the rock record with improved proof of life awaiting new analytical capabilities.

4. Conclusions

We reconfirm the original claim by Nutman et al. (2016) that the proposed Isua stromatolites are genuine biogenic structures, based on new data and a re-examination of the outcrops. We demonstrate through detailed mapping that the stromatolites are definitely an outcrop of the ~3700 Ma part of the bedrock geology. Furthermore, they are dominated by dolomite that contains clear REE+Y seawater-like signatures and carbonate $\delta^{13}C_{VPDB}$ signatures of ~+1‰, identical to common biomediated marine carbonates throughout Earth’s history. Critically, they have structures that match a syn-sedimentary biogenic origin and that cannot be explained by tectonic folding or by soft-sedimentary deformation processes. For all four criteria presented in the Introduction of this paper, the stromatolites *do not* match artefacts produced by post depositional metamorphic, metasomatic and tectonic processes. The data from well-preserved parts of the outcrop studied in the original paper support biogenicity for the proposed Isua stromatolites.

Acknowledgements

We thank Charley Lineweaver for feedback on an earlier draft of this manuscript and the comments of three formal reviewers. This work was supported by Australian Research

Council grant DP170100715. This is contribution xxyy of the Australian Research Council Centre for Excellence for Core to Crust Fluid Systems.

Appendix

Methods LA-Q-ICP-MS

In situ major- and trace-element analyses of polished dolomite thin sections were undertaken by laser ablation (193 nm excimer, ESI NWR 193™), coupled to a quadrupole ICP-MS (iCAP™) at the Wollongong Isotope Geochronology Laboratory, University of Wollongong. Data were acquired for 44 masses using a spot size of 80 µm, 1.42 J/cm^2, 5 µm depth, and 30 Hz with a 650 mL/min He flow. Acquisition time was set to 200 s and blank intensities were measured on the carrier gas for 60 s prior to ablation and subtracted from the mean count rate. Dwell time varied from 0.01 – 0.35 ms, depending on the relative abundance of each analysed mass. Glass reference materials NIST 610, 612, and 615 were used as calibration standards (Norman et al., 1998; Norman et al., 2004) and the data were normalised to the Sr content of an in-house matrix-matched carbonate sample G17/40. Samples were analysed in two sessions and the Sr concentration of the first and second session yielded 116.4 ± 4.5 ppm (2SE, n = 9) and 102.7 ± 5.7 ppm (2SE, n = 9), respectively. Prior to laser ablation measurements, the Sr concentration of G17/40 was determined on chemically dissolved sample aliquots where the solution yielded a Sr concentration of 55.4 ± 14.0 ppm (2SE, n = 3). A commercial laboratory reported a Sr concentration of 65.5 ppm, whereas analysis with a hand-held Niton XRF yielded a Sr concentration of 65 ppm. All major and trace concentration data determined via laser ablation in this study were normalised to the G17/40 Sr content of 65.5 ppm. Quality control for each analytical session was achieved by measuring NIST 612 and G17/40 after every 5th sample and no systematic shift for any of the analytes was observed over an entire session. Small-scale sample heterogeneity was determined by analysing up to 5 carbonate crystals for each sample and the mean value of the normalised major- and trace-element composition is reported in Table 1. Samples that yielded significantly higher Si, Ti and Zr contents were excluded in deriving mean values as these are more likely to contain a terrigenous component.

References

Allaart, J.H., 1976. The pre-3760 m.y. old supracrustal rocks of the Isua area, central West Greenland, and the associated occurrence of quartz-banded ironstone. In: B.F. Windley (Editor), The Early History of the Earth. Wiley, London, pp. 177-189.

Alleon, J., Bernard, S., Le Guillou, C., Beyssac, O., Sugitani, K., Robert, F., 2018. Chemical nature of the 3.4 Ga Strelley Pool microfossils. Geochemical Perspective Letters 7, 37-42 doi: 10.7185/geochemlet.1817

Allwood, A. C., Walter, M. R., Kamber, B. S., Marshall, C. P., Burch, I. W., 2006. Stromatolite reef from the Early Archaean era of Australia. Nature 441, 714-717.

Allwood, A.C., Kamber, B.S., Walter, M.R., Burch, I.W., Kanik, I., 2010. Trace elements record depositional history of an Early Archean stromatolitic carbonate platform. Chemical Geology 270, 148-163.

Allwood, A.C., Rosing, M.T., Flannery, D.T., Hurowitz, J.A., Heirwegh, C.M., 2018. Reassessing evidence of life in 3,700-million-year-old rocks of Greenland. Nature https://doi.org/10.1038/s41586-018-0610-4

Appel, P.W.U., Fedo, C.M., Moorbath, S., Myers, J.S., 1998. Recognizable primary volcanic and sedimentary features in a low-strain domain of the highly deformed, oldest known (≈ 3.7-3.8 Gyr) Greenstone Belt, Isua, West Greenland. Terra Nova 10, 57-62.

Appel, P.W.U., Moorbath, S., Myers, J.S., 2003. Isuasphaera isua (Phlug) revisited. Precambrian Research 126, 309-312.

Awramik, S.M., Grey, K., 2005. Stromatolites: biogenicity, biosignatures and bioconfusion. Proc. SPIE 5906, Astrobiology and Planetary Missions 59060P; doi: 10.1117/12.625556

Baadsgaard, H., 1983. U-Pb isotope systematics on minerals from the gneiss complex at Isukasia, West Greenland. Rapport Grønlands Geologiske Undersøgelse 112, 35-42.

Bau, M., 1999. Scavenging of dissolved yttrium and rare earths by precipitating iron oxyhydroxide; experimental evidence for Ce oxidation, Y-Ho fractionation, and lanthanide tetrad effect. Geochimica et Cosmochimica Acta 63, 67-77.

Bau, M., Dulski, P., 1996. Distribution of Y and rare-earth elements in the Penge and Kuruman Iron Formations, Transvaal Supergroup, South Africa. Precambrian Research 79, 37-55.

Betts, H.C., Puttick, M.N., Clark, J.W., Williams, T.A., Donoghue, P.C.J., Pisani, D., 2018. Integrated genomic and fossil evidence illuminates life's early evolution and eukaryote origin. Nature Ecology and Evolution 2, 1556-1562.

Bolhar, R., Kamber, B.S., Moorbath, S., Fedo, C.M., Whitehouse, M.J., 2004. Characterisation of early Archaean chemical sediments by trace element signatures. Earth Planetary Science Letters 222, 43–60.

Bolhar, R., Kamber, B.S., Moorbath, S., Whitehouse, M.J., Collerson, K.D., 2005. Chemical characterization of earth's most ancient clastic metasediments from the Isua Greenstone Belt, southern West Greenland. Geochimica et Cosmochimica Acta, 69, 1553-1573.

Boak J., Dymek R.F.. 1982. Metamorphism of the ca. 3800 Ma supracrustal rocks at Isua, West Greenland: implications for early Archaean crustal evolution. Earth and Planetary Science Letters 59,155–176. doi: http://dx.doi.org/10.1016/0012-821X(82)90123-6

Bower, D.M., Stelle, A., Fried, M.D., Green, O.R., Lindsay, J.F., 2016. Raman imaging spectroscopy of a putative microfossils from the ~3.46 Ga Apex Chert: Insights from quartz grain orientation. Astrobiology 16, doi:10.1089/ast.2014.1207.

Brasier, M.D., Green, O.R., Jephcoat, A.P., Kleppe, A.K., Van Kranendonk, M.J., Lindsay, J.F., Steele, A., & Grassineau, N. (2002): Questioning the evidence for Earth's oldest fossils. Nature, 416, 76-81.

Brasier, M.D., Green, O.R., Lindsay, J.F., McLoughlin, N., Steele, A., Stokes, C., 2005. Critical testing of Earth's oldest putative fossil assemblage from the ~3.5 Ga Apex chert, Chinaman Creek, Western Australia. Precambrian Research 140, 55-102.

Bridgwater, D., McGregor, V.R., 1974. Field work on the very early Precambrian rocks of the Isua area, southern West Greenland. Rapport Grønlands Geologiske Undersøgelse 65, 49-54.

Bridgwater, D., Allaart, J.H., Schopf, J.W., Klein, C., Walter, E.S., Strother, P., Knoll, A.H., Gorman, B.E., 1981. Microfossil-like objects from the Archaean of Greenland: a cautionary note. Nature 289, 51–53.

Brocks, J.J., Love, G.D., Summons, R.E., Knoll, A.H., Logan, G.A., Bowden, S.A., 2005. Biomarker evidence for green and purple sulphur bacteria in a stratified Palaeoproterozoic sea. Nature 437, 866-870.

Buick, R., Dunlop, J.S.R., Groves, D.I., 1981. Stromatolite recognition in ancient rocks: an appraisal of irregular laminated structures in an early Archaean chert-barite unit from North Pole, Western Australia. Alcheringa 5, 161-181.

Compston, W., Kinny, P.D., Williams, I.S., Foster, J.J., 1986. The age and lead loss behaviour of zircons from the Isua supracrustal belt as determined by ion microprobe. Earth and Planetary Science Letters 80, 71-81.

Craddock, P.R., Dauphas, N., 2011. Iron and carbon isotope evidence for microbial iron respiration throughout the Archean. Earth and Planetary Science Letters 303, 121–132.

Crowley, J.L., 2003. U-Pb geochronology of 3810-3630 Ma granitoid rocks south of the Isua greenstone belt, southern West Greenland. Precambrian Research 126, 235-257.

Crowley, J.L., Myers, J.S., Dunning, G.R., 2002. Timing and nature of multiple 3700-3600 Ma tectonic events in intrusive rocks north of the Isua greenstone belt, southern West Greenland. Geological Society of America Bulletin 114, 1311-1325.

Darling, J.R., Moser, D.E., Heaman, L.H., Davis, W.J., O'Neil, J., Carlson, R., 2013. Eoarchean to Neoarchean evolution of the Nuvvuagittuq Supracrustal belt: New insights from U-Pb zircon geochronology. American Journal of Science 313, 844-876.

Dauphas, N., van Zuilen, M., Wadhwa, M., Davis, A.M., Marty, B., Janney, P.E., 2004. Clues from Fe isotope variations on the origin of early Archaean BIFs from Greenland. Science 306, 2077–2080.

Dymek, R.F. and Klien, C., 1988. Chemistry, petrology and origin of banded iron-formation lithologies from the 3800 Ma Isua supracrustal belt, west Greenland. Precambrian Research 39, 247-302.

Fedo, C.M., 2000. Setting and origin of problematic rocks from the >3.7 Ga Isua greenstone belt, southern West Greenland: Earth's oldest coarse clastic sediments. Precambrian Research 101, 69-78.

Flannery, D., Allwood, A.C., Van Kranendonk, M.J., 2016. Lacustrine facies dependence of highly ^{13}C-depleted organic matter during the global age of methanotrophy. Precambrian Research 285, 216-241.

French, K.L., Hallmann, C., Hope, J.M., Schoon, P.L., Zumberge, J.A., Hoshino, Y., Peters, C.A., George, S.C., Love, G.D., Brocks, J.J., Buick, R., Summons, R.E., 2015. Reappraisal of hydrocarbon biomarkers in Archean rocks. PNAS 112, 5915-5920.

Friend, C.R.L., Bennett, V.C., Nutman, A.P., Norman, M.D. 2007. Seawater-like trace element signatures (REE + Y) of Eoarchaean chemical sedimentary rocks from southern West Greenland, and their corruption during high-grade metamorphism. Contributions to Mineralogy and Petrology 155, 229-246.

Furnes, H., de Wit, M., Staudigel, H., Rosing, M., Muehlenbachs, K., 2007. Vestige of Earth's oldest ophiolite. Science 215, 1704-1707.

Grotzinger, J. P., Knoll, A. H., 1999. Stromatolites in Precambrian carbonates: Evolutionary mileposts or environmental dipsticks? Annual Review of Earth and Planetary

Sciences, 27, 313–358. https://doi.org/10.1146/annurev.earth.27.1.313

Hanmer, S., Greene, D.C., 2002. A modern structural regime in the Paleoarchean (~3.64 Ga); Isua Greenstone Belt, southern West Greenland. Tectonophysics 346, 201-222.

Hassenkam, T., Andersson, M.P., Dalby, K.N., Mackenzie, D.M.A., Rosing, M.T., 2017. Elements of Eoarchean life trapped in mineral inclusions. Nature 548, 78–81.

Hofmann, H. J., Grey, K., Hickman, A. H., and Thorpe, R., 1999, Origin of 3.45 Ga coniform stromatolites in the Warrawoona Group, Western Australia. Geological Society of America Bulletin 111, 1256-1262.

Jenner, F.E., Bennett, V.C., Nutman, A.P., Friend, C.R.L., Norman, M.D., Yaxley, G. 2009. Evidence for subduction at 3.8 Ga: Geochemistry of arc-like metabasalts from the southern edge of the Isua Supracrustal Belt. Chemical Geology 261, 83-98.

Kalkowsky, E., 1908. Oolith und Stromatolith im norddeutschen Buntsandstein. Zeitschrift derdeutschen geologischen Gesellschaft 60, 68–125.

Kamber, B. S., Whitehouse, M. J., Bolhar, R., Moorbath, S., 2005. Volcanic resurfacing and the early terrestrial crust: Zircon U-Pb and REE constraints from the Isua Greenstone Belt, southern West Greenland. Earth and Planetary Science Letters 240, 276-290.

Kamber, B.S., Webb, G.E., Gallagher, M., 2014. The rare earth element signal in Archaean microbial carbonate: information on ocean redox and biogenicity. Journal of the Geological Society, London 171, 745-763.

Komiya, T., Maruyama, S., Masuda, T, Appel., P.W.U., Nohda, S., 1999. The 3.8-3.7 Ga plate tectonics on the Earth; Field evidence from the Isua accretionary complex, West Greenland. Journal of Geology 107, 515-554.

Krumbein, W. E., 1983. Stromatolites – the challenge of a term in space and time. Precambrian Research, 20, 493–531.

Lepot, K., Benzerara, K., Brown, G.E., Philipott, P., 2008. Microbially influenced formation of 2,724-million-year-old stromatolites. Nature Geoscience doi:10.1038/ngeo107

Myers, J.S., 2001. Protoliths of the 3.8–3.7 Ga Isua greenstone belt, West Greenland. Precambrian Research 105, 129-141.

Norman, M., Griffin, W., Pearson, N., Garcia, M., O'Reilly, S., 1998. Quantitative analysis of trace element abundances in glasses and minerals: a comparison of laser ablation inductively coupled plasma mass spectrometry, solution inductively coupled plasma mass spectrometry, proton microprobe and electron microprobe data. Journal of Analytical Atomic Spectrometry 13, 477-482.

Norman, M. D., Garcia, M. O., Bennett, V.C., 2004. Rhenium and chalcophile elements in basaltic glasses from Ko'olau and Moloka'i volcanoes: Magmatic outgassing and composition of the Hawaiian plume. Geochimica et Cosmochimica Acta 68, 3761-3777.

Nutman, A.P., 1986. The geology of the Isukasia region, southern West Greenland. Grønlands geologiske Undersøgelse Bulletin 154, 80 pp.

Nutman, A.P., Collerson, K.D., 1991. Very early Archean crustal-accretion complexes preserved in the North Atlantic Craton. Geology 19, 791-795.

Nutman, A.P., Friend, C.R.L., 2009. New 1:20000 geological maps, synthesis and history of the Isua supracrustal belt and adjacent gneisses, Nuuk region, southern West Greenland: A glimpse of Eoarchaean crust formation and orogeny. Precambrian Research 172, 189-211.

Nutman, A.P., Allaart, J.H., Bridgwater, D. Dimroth, E., Rosing, M.T., 1984. Stratigraphic and geochemical evidence for the depositional environment of the early Archaean Isua supracrustal belt, southern West Greenland. Precambrian Research 25, 365-396.

Nutman, A.P., McGregor, V.R., Friend, C.R.L., Bennett, V.C., Kinny, P.D., 1996. The Itsaq Gneiss Complex of southern West Greenland; the world's most extensive record of early crustal evolution (3900-3600 Ma). Precambrian Research 78, 1-39.

Nutman, A.P., Bennett, V.C., Friend, C.R.L., Rosing, M.T., 1997. ~3710 and ≥3790 Ma volcanic sequences in the Isua (Greenland) supracrustal belt; structural and Nd isotope implications. Chemical Geology 141, 271-287.

Nutman, A.P., Bennett, V.C., Friend, C.R.L., Norman, M.D., 1999. Meta-igneous (non-gneissic) tonalites and quartz-diorites from an extensive ca. 3800 Ma terrain south of the Isua supracrustal belt, southern West Greenland: Constraints on early crust formation. Contributions to Mineralogy and Petrology 137, 364-388.

Nutman, A.P., Friend, C.R.L., Bennett, V.C., McGregor, V.R., 2000. The early Archaean Itsaq Gneiss Complex of southern West Greenland: The importance of field observations in interpreting dates and isotopic data constraining early terrestrial evolution. Geochimica et Cosmochimica Acta 64, 3035-3060.

Nutman, A.P., Friend, C.R.L., Bennett, V.C., 2002. Evidence for 3650-3600 Ma assembly of the northern end of the Itsaq Gneiss Complex, Greenland: Implication for early Archean tectonics. Tectonics 21, article 5.

Nutman, A.P., Friend, C.R.L., Paxton, S., 2009. Detrital zircon sedimentary provenance ages for the Eoarchaean Isua supracrustal belt, southern West Greenland: Juxtaposition of an imbricated ca. 3700 Ma juvenile arc assemblage against an older complex with 3920-3800 Ma components. Precambrian Research 172, 212-233.

Nutman, A.P., Friend, C.R.L., Bennett, V.C., Wright, D., Norman, M.D., 2010. ≥3700 Ma pre-metamorphic dolomite formed by microbial mediation in the Isua supracrustal belt (W. Greenland): Simple evidence for early life? Precambrian Research 183, 725-737.

Nutman, A.P., Bennett, V.C., Friend, C.R.L., Van Kranendonk, M., Chivas, A.R., 2016. Rapid emergence of life shown by discovery of 3,700 million year old microbial structures. Nature 537, 535-537.

Nutman, A.P., Bennett, V.C., Friend, C.R.L., Chivas, A.R., 2017. The Isua supracrustal belt of the North Atlantic Craton (Greenland): Spotlight on sedimentary systems with the oldest-preserved sedimentary structures (~3.7, ~3.75 and ~3.8 Ga). In: Muzumder, R. (ed) Sediment Provenance: Influences in Compositional Change from Source to Sink, Elsevier, pp. 563-592. DOI 10.1016/B978-0-12-803386-9.00020-4.

Perry, E.C., Ahmad, S.N., 1977. Carbon isotope composition of graphite and carbonate minerals from 3.8 Æ metamorphosed sediments, Isukasia, Greenland. Earth and Planetary Science Letters 36, 280-284.

Pflug, H.D., Jaeschke-Boyer, H., 1979. Combined structural and chemical analysis of 3,800-Myr-old microfossils. Nature 280, 483−486.

Polat, A., Hofmann, A.W., 2003. Alteration and geochemical patterns in the 3.7-3.8 Ga Isua greenstone belt, West Greenland. Precambrian Research 126, 197-218.

Polat, A., Hofmann, A.W., Rosing, M.T. 2002. Boninite-like volcanic rocks in the 3.7-3.8 Ga Isua greenstone belt, West Greenland: geochemical evidence for intra-oceanic subduction zone processes in the early Earth. Chemical Geology 184, 231-254.

Ramsay, J.G. Huber, M.I., 1987. The Techniques of Modern Structural Geology Volume 2: Folds and Fractures. Elsevier Science Ltd., Amsterdam.

Reid, R.P., Visscher, P.T., Decho, A.W., Stolz, J.F., Bebout, B.M., Dupraz, C., MacIntyre, I.G., Paerl, H.W., Pinckney, J.L., Prufert-Bebout, L., Steppe, T.F., Des Marais, D.J., 2000. The role of microbes in accretion, lamination and early lithification of modern marine stromatolites. Nature, 406, 989–992.

Riding, R., 2011. The nature of stromatolites: 3,500 million years of history and a century of research. In: J.Reitner et al. (editors) Advances in Stromatolite Geobiology, Springer-Verlag, Berlin, 29-74.

Roberts, J.A., Bennett, P.C., González, L.A., Macpherson, G.L., Milliken, K.L., 2004. Microbial precipitation of dolomite in methanogenic groundwater. Geology 32, 277-280.

Rollinson, H., 2003. Metamorphic history suggested by garnet-growth chronologies in the Isua Greenstone Belt, West Greenland. Precambrian Research 126, 181–196.

Rose, N.M., Rosing, M.T., Bridgwater, D., 1996. The origin of metacarbonate rocks in the Archaean Isua supracrustal belt, West Greenland. American Journal of Science 296, 1004-1044.

Rosing, M.T., 1999. ^{13}C-depleted carbon microparticles in >3700 Ma sea-floor sedimentary rocks from West Greenland. Science 283, 674-676.

Rosing, M.T., Rose, N.M., Bridgwater, D., Thomsen, H.S., 1996. Earliest part of Earth’s stratigraphic record: A reappraisal of the >3.7 Ga Isua (Greenland) supracrustal sequence. Geology 24, 43-46.

Schidlowski, M., 2001. Carbon isotopes as biogeochemical recorders of life over 3.8 Ga of Earth history: evolution of a concept. Precambrian Research 106, 117-134.

Schidlowski, M. Appel, P.W.U., Eichmann, R., Junge, C.E., 1979. Carbon isotope geochemistry of the 3.7 x 10^9 –yr old Isua sediments, West Greenland: implications for the Archaean carbon and oxygen cycles. Geochimica et Cosmochimica Acta 43, 189-199.

Schopf, J.W., 1993. Microfossils of the Early Archaean Apex Chert: new evidence of the antiquity of life: Science, 260, 640-646.

Schopf, J.W., Kitajima, K., Spicuzza, M.J., Kudryatsev, A.B., Valley, J.W., 2017. SIMS analyses of the oldest known assemblage of microfossils document their taxon-correlated carbon isotope compositions. PNAS, DOI:10.1073/pnas.1718063115.

Skippen, G.B., 1974. An experimental model for the low pressure metamorphism of siliceous dolomitic marble. American Journal of Science 274, 487-509.

Solvang, M., 1999. An investigation of metavolcanic rocks from the eastern part of the Isua greenstone belt, West Greenland. Geological Survey of Denmark and Greenland (GEUS) Internal Report, Copenhagen, Denmark, 62 pages.

Stüeken, E.E., 2016. Nitrogen in ancient mud: A biosignature. Astrobiology 16, No. 9, doi.org/10.1089/ast.2016.1478

Walter, M. R., 1976. Introduction. In: Walter, M. R. (ed.), Stromatolites. Developments in Sedimentology, 20, 1–3. Amsterdam: Elevier.

Wright, D. T., Oren, A., 2005. Non-photosynthetic bacteria and the formation of carbonates and evaporites through time. Geomicrobiology Journal 22, 27-53.

Wright, D.T., Wacey, D., 2005. Precipitation of dolomite using sulphate-reducing bacteria from the Coorong Region, South Australia: significance and implications. Sedimentology 52, 987-1008.

Van Kranendonk, M.J., 2006. Volcanic degassing, hydrothermal circulation and the flourishing of early life on Earth: a review of the evidence from c. 3490-3240 Ma rocks of the Pilbara Supergroup, Pilbara Craton, Western Australia. Earth-Science Reviews 74, 197-240.

Van Kranendonk, M.J., 2011. Stromatolite morphology as an indicator of biogenicity for Earth's oldest fossils from the 3.5-3.4 Ga Pilbara Craton, Western Australia. In: Advances in Stromatolite Geobiology, edited by J. Reitner, N-V. Queric, and G. Arp. Lecture Notes in Earth Sciences, 131, Springer, Germany, pp. 517–534.

Van Kranendonk, M.J., Webb, G.E., Kamber, B.S., 2003. Geological and trace element evidence for a marine sedimentary environment of deposition and biogenicity of 3.45 Ga stromatolitic carbonates in the Pilbara Craton, and support for a reducing Archaean ocean. Geobiology 1, 91–108.

Vasconcelos, C., McKenzie, J.A., Bernasconi, S., Grujic, D., Tien, A.J., 1995. Microbial mediation as a possible mechanism for natural dolomite at low temperatures. Nature 377, 220-222.

Veizer, J., Hoefs, J., 1976. The nature of O^{18}/O^{16} and C^{13}/C^{12} secular trends in sedimentary carbonate rocks. Geochimica et Cosmochimica Acta 40, 1387-1395.

Table Captions

Table 1. Trace element chemical analyses of stromatolite carbonates and associated sedimentary rocks.

Figure captions

Figure 1. Geological map encompassing a northeastern part of the Isua supracrustal belt (after Nutman and Friend, 2009).

Figure 2. (a) Detailed geological map of where the proposed ~3700 Ma stromatolites (sites labelled ‘A’ and ‘B’) occur. ‘D’ refers to dolomite-bearing cross-bedded sandstones shown in Figure 11b. (b) The ‘A’ and ‘B’ outcrops, viewed from the northwest. The outcrops were until recently covered by a perennial snowpatch, the border of which is indicated.

Figure 3. (a, b) Sampled proposed stromatolite site ‘A’ from Nutman et al. (2016) showing internal mm-scale layering (l) (overprinted by a recrystallisation domain (x)), that is bowed relative to the flat layering at the stromatolite’s base and in overlying layers (f), the white horizontal arrow indicates thin layer discussed in section 3.4. Saw cuts are preliminary stages in obtaining our sample. Blue lines indicate the trend of the weak mica foliation, at a high angle to the bedding. (c, d) More deformed and altered southwestern end of same outcrop – the focus of Allwood et al. (2018). Red arrows highlight example areas where secondary,

dark brown carbonate veins cut across beds labelled B and C, which underlie the stromatolite horizon, as well as the stromatolites (S). These veins are absent from the better-preserved part of the same outcrop studied by Nutman et al. (2016). The apparent "upside-down" structure 'A' is a remnant of a once laterally continuous bed, now cut on both sides by the secondary carbonate.

Figure 4. Cartoon demonstrating the deformation geometry in Isua folds. Note that although stretching is prevalent in a steeply plunging orientation, relict (sedimentary and volcanic) features can still survive in the other two dimensions in fold core / hinge region.

Figure 5. Intercrystalline fluid composition (XCO_2 versus XH_2O) versus temperature (at 2 kb confining pressure) for compositions expressed as quartz + dolomite at low temperature. *tr+cc* = is the lowest-temperature tremolite-producing reaction (after Skippen, 1974).

Figure 6. (a) Scanning electron microscope (SEM) image of metamorphic (550-500°C) granoblastic equilibrium texture of quartz (qtz) + dolomite (dol) with Mg-rich biotite (phl) preserved in Isua ~3700 Ma stromatolite rock. Note the complete lack of reaction along the quartz-dolomite grain boundaries (no tremolite growth). (b) Pilbara Craton (Australia) Paleoarchean Strelley Pool Chert Formation stromatolites (21°11.797'S 119°18.421'E; GPS datum WGS84), showing extensive granoblastic recrystallisation (rex) that obliterates their original layering (lay). This is despite these rocks were subjected to much lower metamorphic temperatures (≤300°C) than at Isua.

Figure 7. The Nutman et al. (2016) site 'A' (within the red line). Note the continuity of its rock type and orientation of its layering with the adjacent outcrops, where the darker colour indicates the start of extensive tremolite development by reaction between quartz and dolomite.

Figure 8. (a) Centre – kernel of finely-layered dolomite and quartz rock <10 m from site ‘A’ stromatolites. Surrounding – coarse-grained rock with tremolite development – this secondary fluid-mediated recrystallisation is clearly overprinting and destroying the original fine-scale dolomite + quartz layering across a front that is at an angle to the original layering at the ends of the kernel (see close-up of this transition in the top right inset). This shows that the tremolite is late and the dolomite is early. With increased deformation here, compared to where the stromatolites are preserved, note that *all* layers are taking on an undulating form, due to layer-parallel compression. This geometry is absent from the site ‘A’ outcrop nearby. A5 notebook for scale. (b) Anastomosing, discordant magnesite carbonate veins (V) cutting recrystallised and deformed tremolite-rich rocks, with only crude layering surviving, ~25 m south southwest of stromatolite locality ‘A’. G17/39 indicates location of vein carbonate sample.

Figure 9. Single-spot analyses of pure dolomite carbonate (strom. dol. (spot)) show the diagnostic seawater-like signature (upward Y spike and strongly downward bowed La-Sm pattern), identical to a short track over aggregates of dolomite grains (strom. dol. (track)). Mica-bearing layers outside the stromatolite (‘dirty’ layer (track) with mica) show degeneration of the seawater-like signature. Magnesite carbonate vein G17/39 cuts tremolite-rich rocks ~25 m south southwest of stromatolite locality ‘A’. Abundance data have been normalised to the Post Archean Average Shale composite (PAAS).

Figure 10. Detailed images of the site ‘A’ and ‘B’ stromatolite occurrences. (a) Site ‘A’ shows the four sides of the sampled block, displayed in order. If the 3D form is still not clear to the reader, we suggest printing the image, cutting around the block’s four side images and folding it to reconstruct the 3D form. A 42 Mb manipulatable 3D pdf of this sample is also available in the supplementary data. The long sides of the block are approximately in the direction of regional ductile stretching. In planes orthogonal to that (on the weathered front of

the block and the back surface) the amount of distortion is minimal (see also Figs. 3a, b and 4). (b) Site ‘B’ shows the smaller scale proposed stromatolite structures as revealed in a thin section. For site ‘A’ LA-ICP-MS indicates the sub-block that was used in the Laser Ablation ICP-MS geochemical traverses presented in Nutman et al. (2016). Coloured lines and ‘S’ on both images indicates overlying onlapping sedimentary bedding and the proposed stromatolites respectively. (c) SEM backscatter imaging over the margin of an ‘A’ stromatolite, where the brightness of tone conveys relative proportions of dolomite and quartz. Note that despite the development of a granoblastic texture with a coarsening of grain size, which over the mapped area there are bands/layers of different dolomite versus quartz content, parallel to the stromatolites margin.

Figure 11. (a) Stromatolite ‘B’ sampling site. The stromatolites (dolo) are succeeded by bedded quartz + dolomite + mica rocks (sst), showing cross-bedding and scouring of the layers. Pen for scale. (b) Cross-bedding in quartz rich, but dolomite-bearing sandstones at ‘D’ on Figure 2a.

Figure 12. Compilation of Isua carbonate and graphite $\delta^{13}C_{VPDB}$ signatures. Apart from the Nutman et al. (2016) dolomites, most carbonates are from strongly-deformed, mostly calc-silicate-bearing rocks collected in the 1970s, when there was less understanding of the Isua geology.

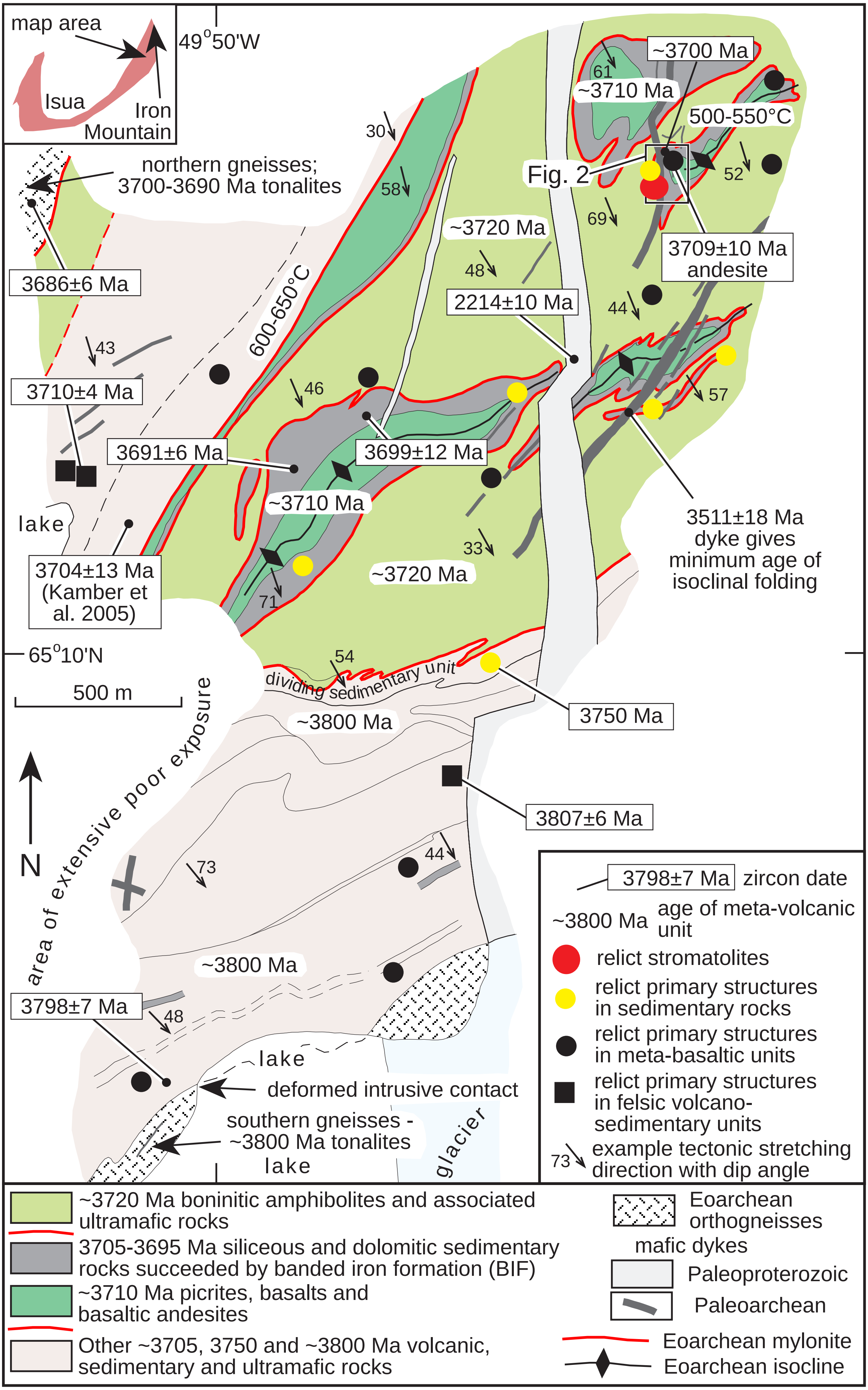
map area
Isua
Iron Mountain
49°50'W
30
58
northern gneisses;
3700-3690 Ma tonalites
3686±6 Ma
600-650°C
43
3710±4 Ma
46
3691±6 Ma
3699±12 Ma
~3710 Ma
lake
3704±13 Ma (Kamber et al. 2005)
71
65°10'N
500 m
~3720 Ma
48
2214±10 Ma
~3720 Ma
33
61
~3710 Ma
~3700 Ma
500-550°C
Fig. 2
52
69
3709±10 Ma andesite
44
57
3511±18 Ma dyke gives minimum age of isoclinal folding
54
dividing sedimentary unit
3750 Ma
~3800 Ma
3807±6 Ma
area of extensive poor exposure
N
73
44
~3800 Ma
3798±7 Ma
48
lake
deformed intrusive contact
southern gneisses - ~3800 Ma tonalites
lake
glacier
3798±7 Ma zircon date
~3800 Ma age of meta-volcanic unit
relict stromatolites
relict primary structures in sedimentary rocks
relict primary structures in meta-basaltic units
relict primary structures in felsic volcano-sedimentary units
73 example tectonic stretching direction with dip angle
~3720 Ma boninitic amphibolites and associated ultramafic rocks
3705-3695 Ma siliceous and dolomitic sedimentary rocks succeeded by banded iron formation (BIF)
~3710 Ma picrites, basalts and basaltic andesites
Other ~3705, 3750 and ~3800 Ma volcanic, sedimentary and ultramafic rocks
Eoarchean orthogneisses
mafic dykes
Paleoproterozoic
Paleoarchean
Eoarchean mylonite
Eoarchean isocline

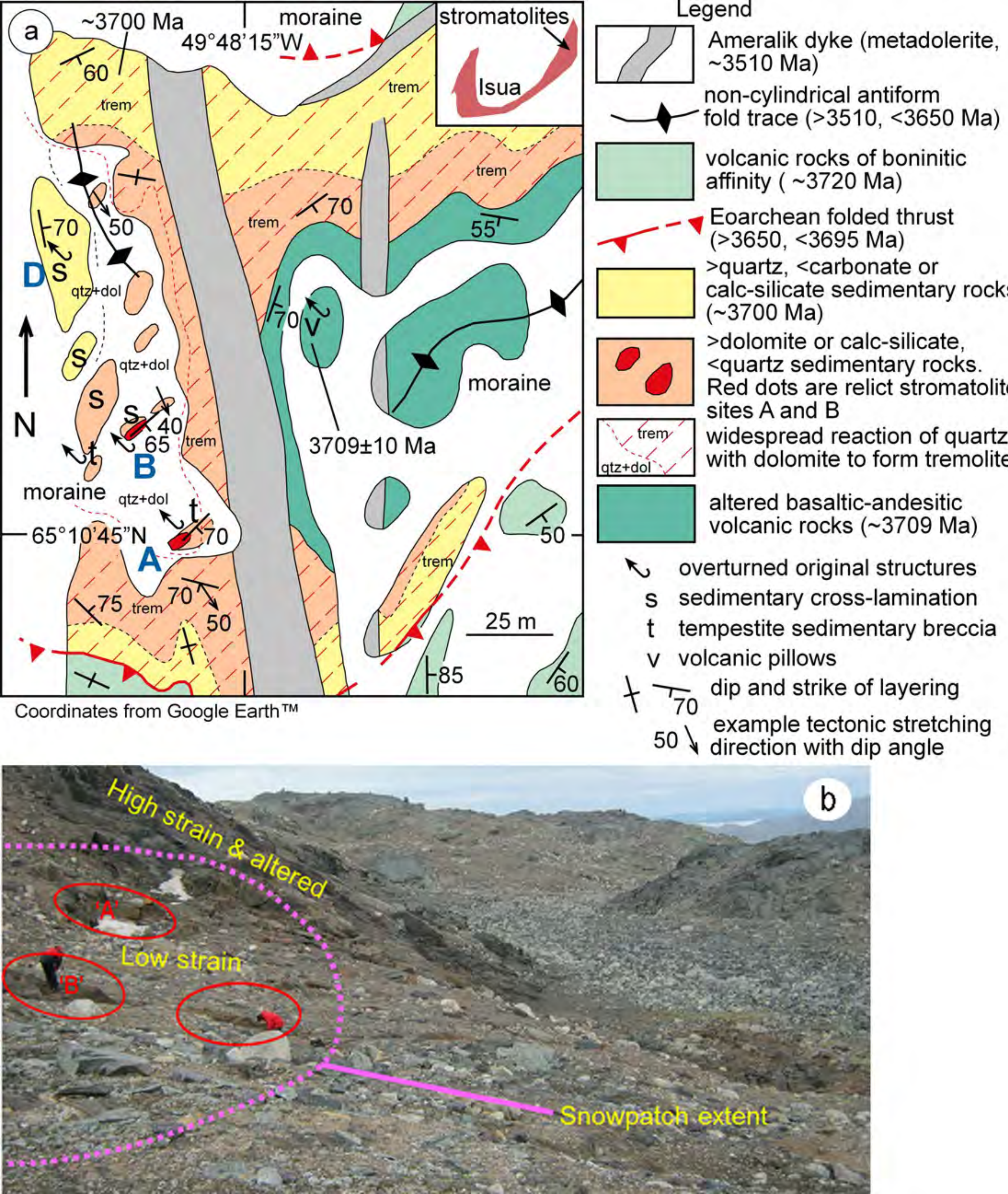

a
~3700 Ma
moraine
49°48'15"W
stromatolites
Isua
trem
qtz+dol
D
N
B
A
moraine
65°10'45"N
3709±10 Ma
25 m
Coordinates from Google Earth™
Legend
Ameralik dyke (metadolerite, ~3510 Ma)
non-cylindrical antiform fold trace (>3510, <3650 Ma)
volcanic rocks of boninitic affinity (~3720 Ma)
Eoarchean folded thrust (>3650, <3695 Ma)
>quartz, <carbonate or calc-silicate sedimentary rocks (~3700 Ma)
>dolomite or calc-silicate, <quartz sedimentary rocks. Red dots are relict stromatolite sites A and B
widespread reaction of quartz with dolomite to form tremolite
altered basaltic-andesitic volcanic rocks (~3709 Ma)
overturned original structures
s sedimentary cross-lamination
t tempestite sedimentary breccia
v volcanic pillows
dip and strike of layering
example tectonic stretching direction with dip angle
b
High strain & altered
'A'
Low strain
'B'
Snowpatch extent

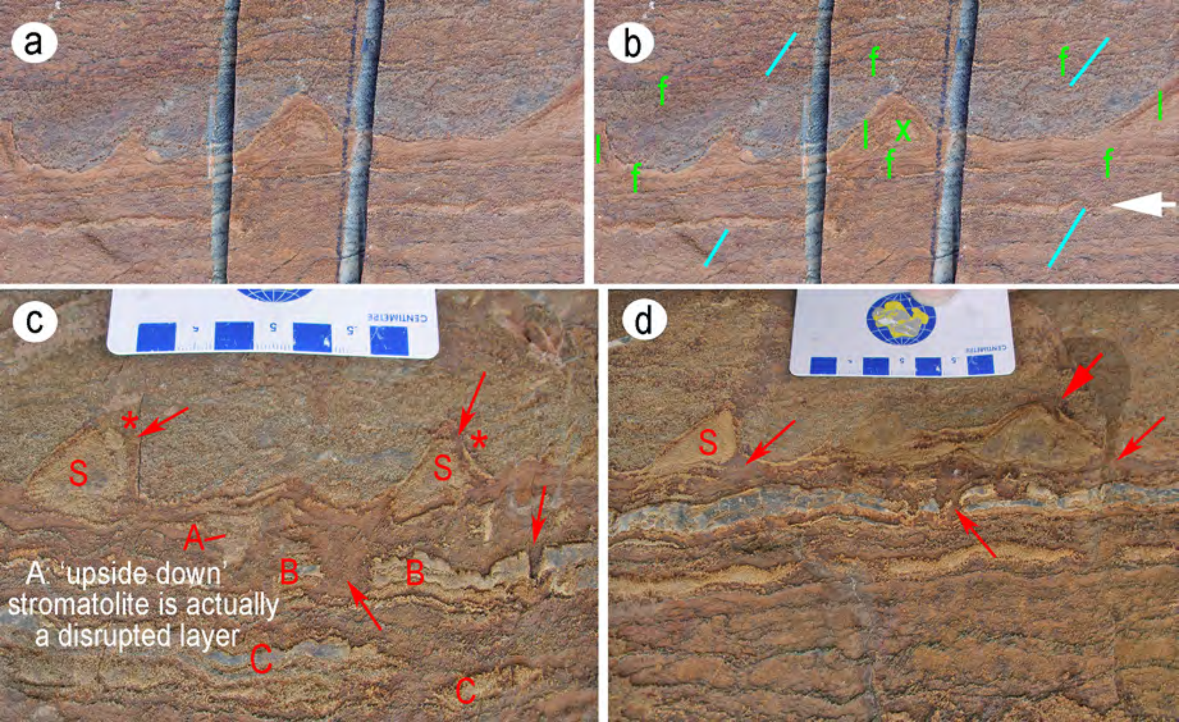
a
b
f
f
f
f
f
f
l
l
l
x
c
d
S
S
S
A
B
B
C
C
A: 'upside down'
stromatolite is actually
a disrupted layer
CENTIMETRE
CENTIMETRE

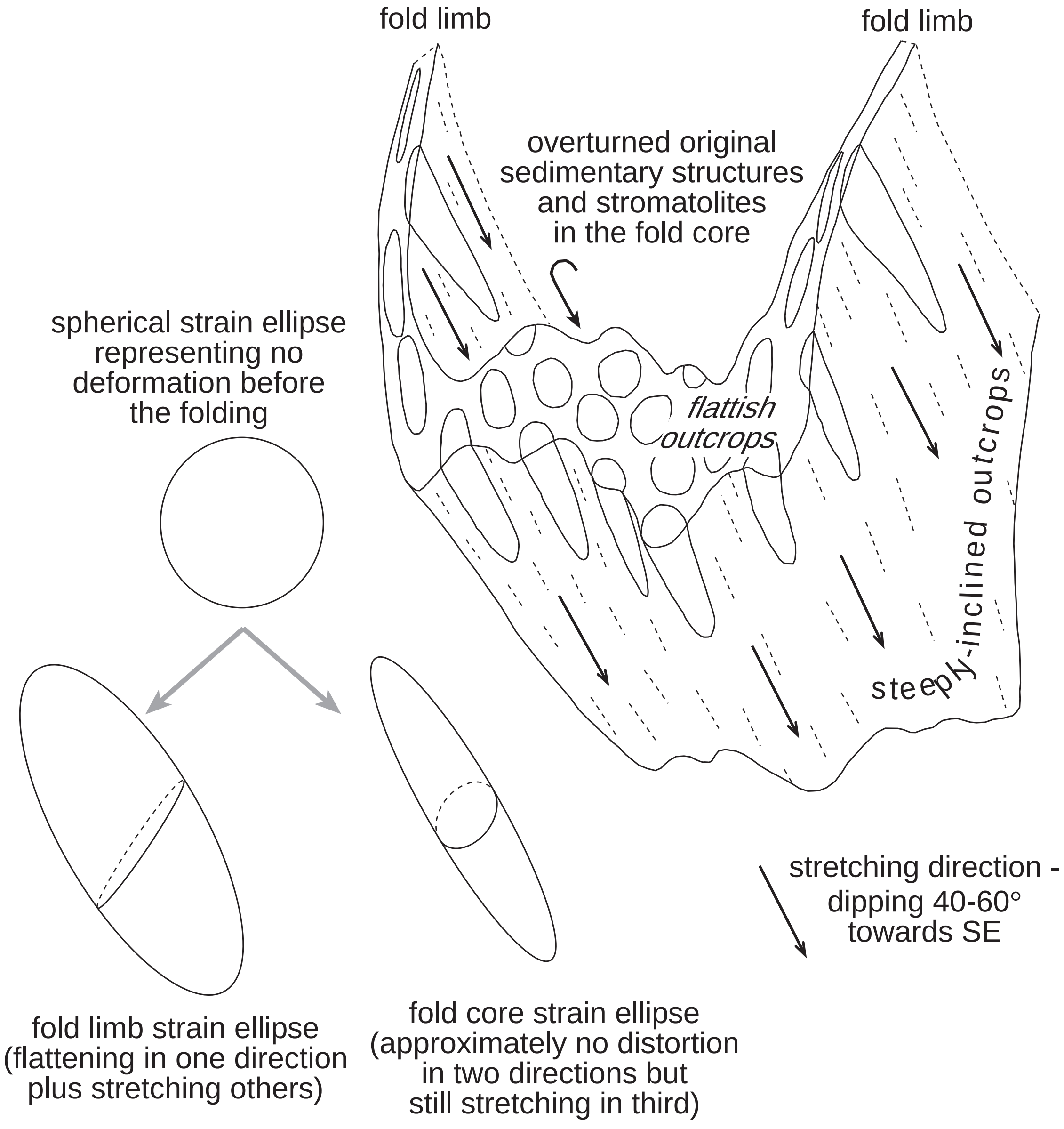
fold limb
fold limb
overturned original sedimentary structures and stromatolites in the fold core
spherical strain ellipse representing no deformation before the folding
flattish outcrops
steeply-inclined outcrops
stretching direction - dipping 40-60° towards SE
fold limb strain ellipse (flattening in one direction plus stretching others)
fold core strain ellipse (approximately no distortion in two directions but still stretching in third)

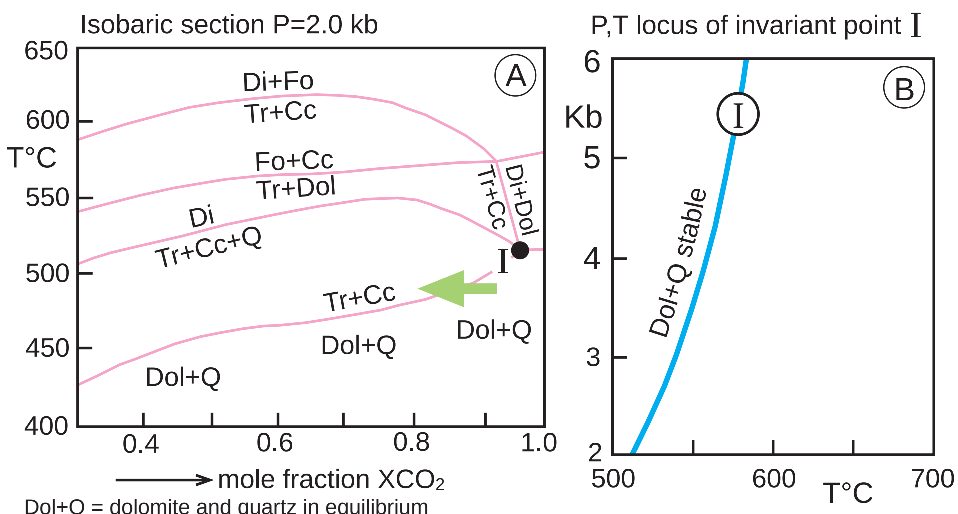

Dol+Q = dolomite and quartz in equilibrium
Cc=calcite, Tr=tremolite, Di=diopside and Fo=forsterite

reaction trigered by adding water
at constant temperature

Impurities (Fe, Mn) will lower
reaction temperatures

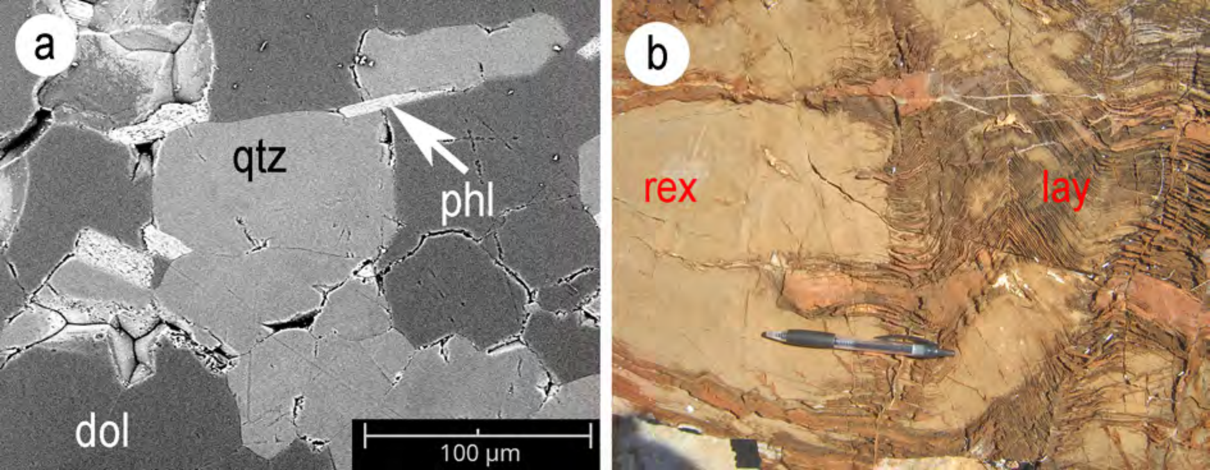
a
qtz
phl
dol
100 µm
b
rex
lay


northern end
of site 'A'

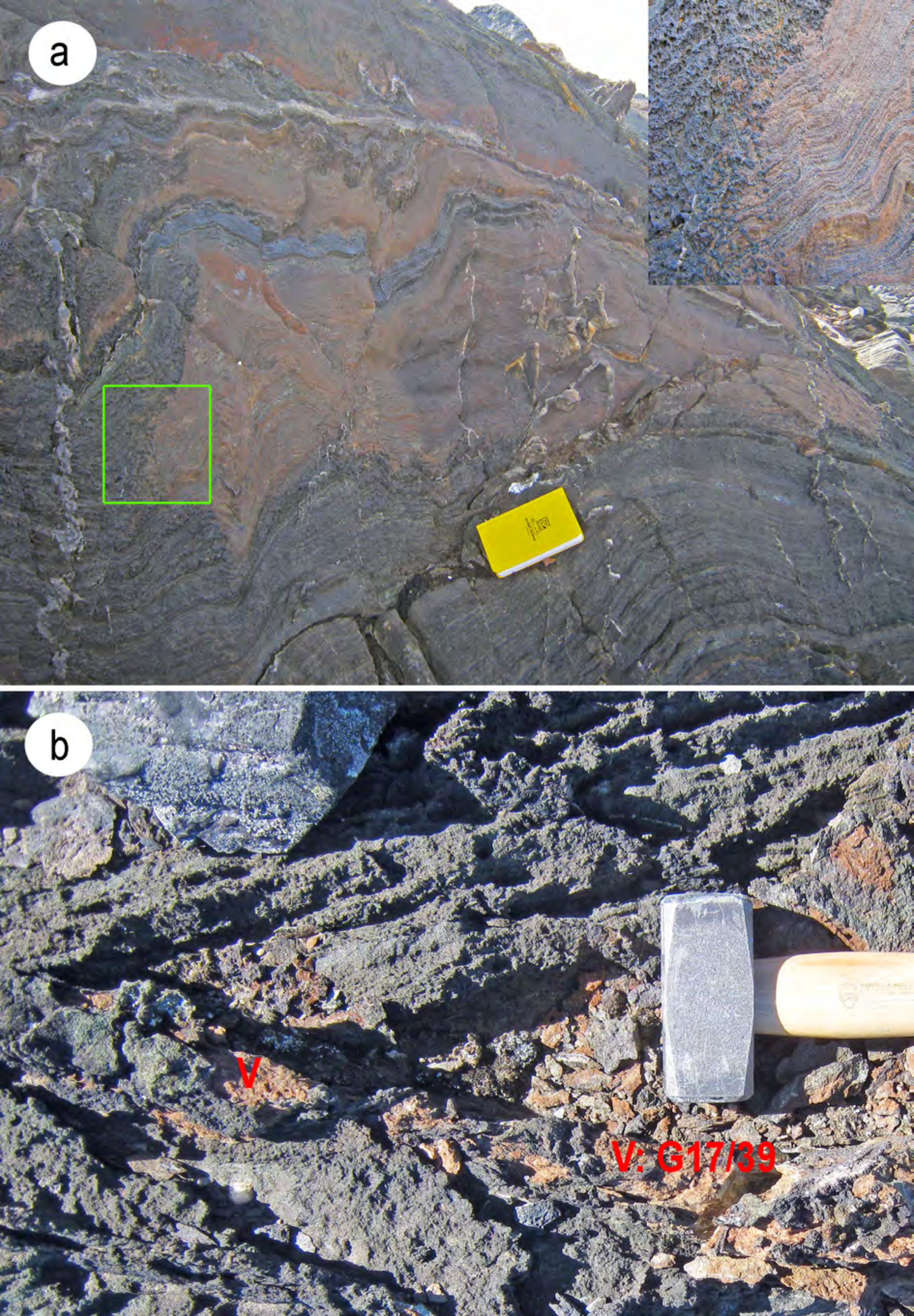
a
b
V
V: G17/39

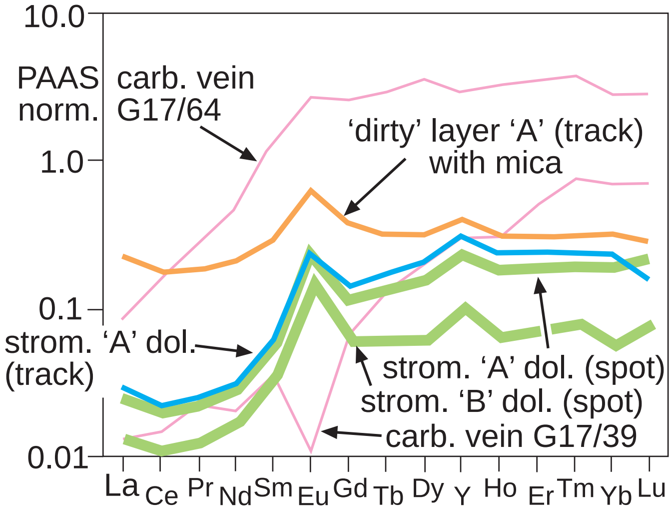

10.0
PAAS norm.
1.0
0.1
0.01
carb. vein G17/64
'dirty' layer 'A' (track) with mica
strom. 'A' dol. (track)
strom. 'A' dol. (spot)
strom. 'B' dol. (spot)
carb. vein G17/39
La
Ce
Pr
Nd
Sm
Eu
Gd
Tb
Dy
Y
Ho
Er
Tm
Yb
Lu

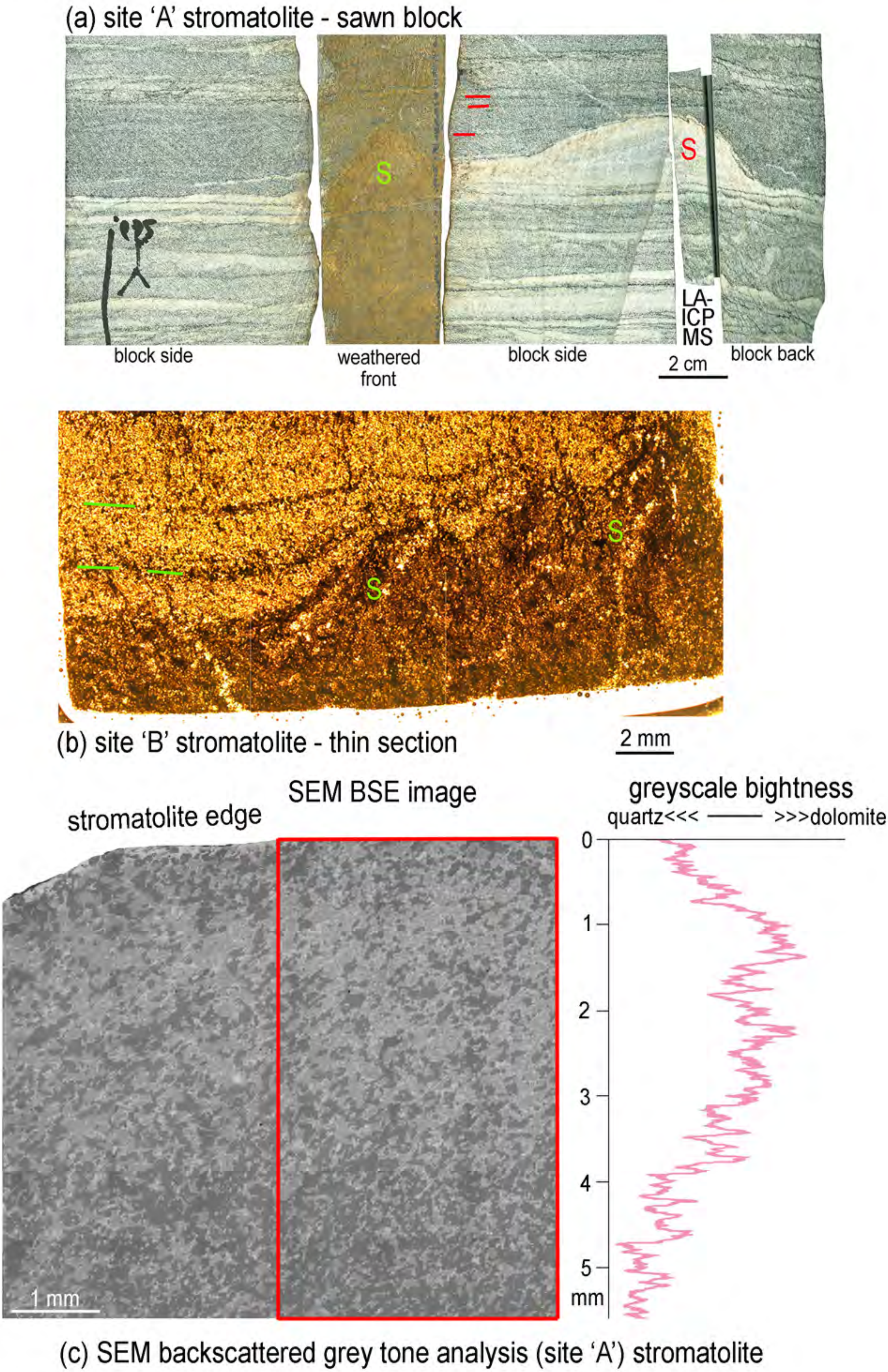
(a) site 'A' stromatolite - sawn block
S
S
LA-ICP MS
block side
weathered front
block side
2 cm
block back
S
S
(b) site 'B' stromatolite - thin section
2 mm
stromatolite edge
SEM BSE image
greyscale bightness
quartz<<< >>>dolomite
0
1
2
3
4
5
mm
1 mm
(c) SEM backscattered grey tone analysis (site 'A') stromatolite

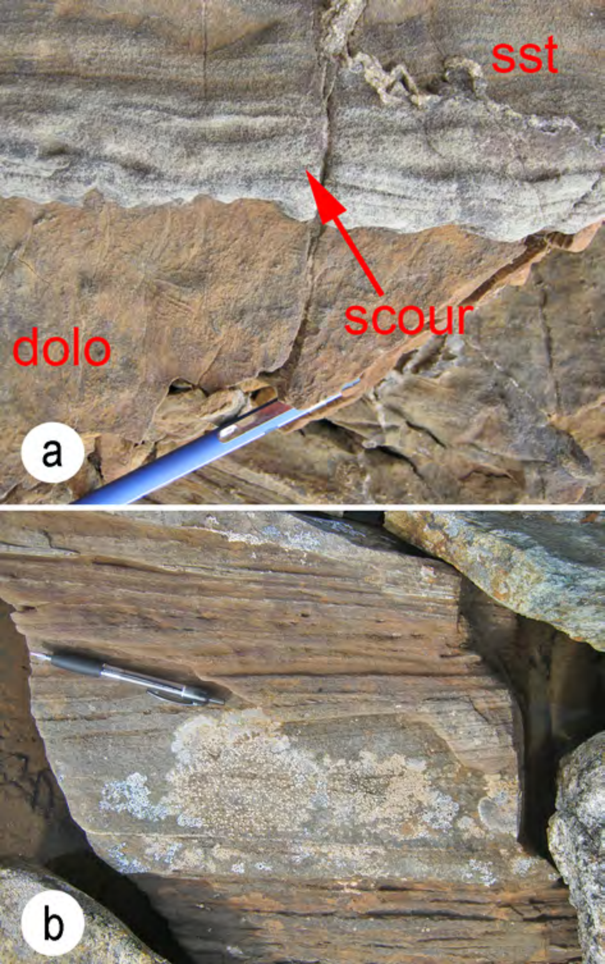
sst
scour
dolo
a
b

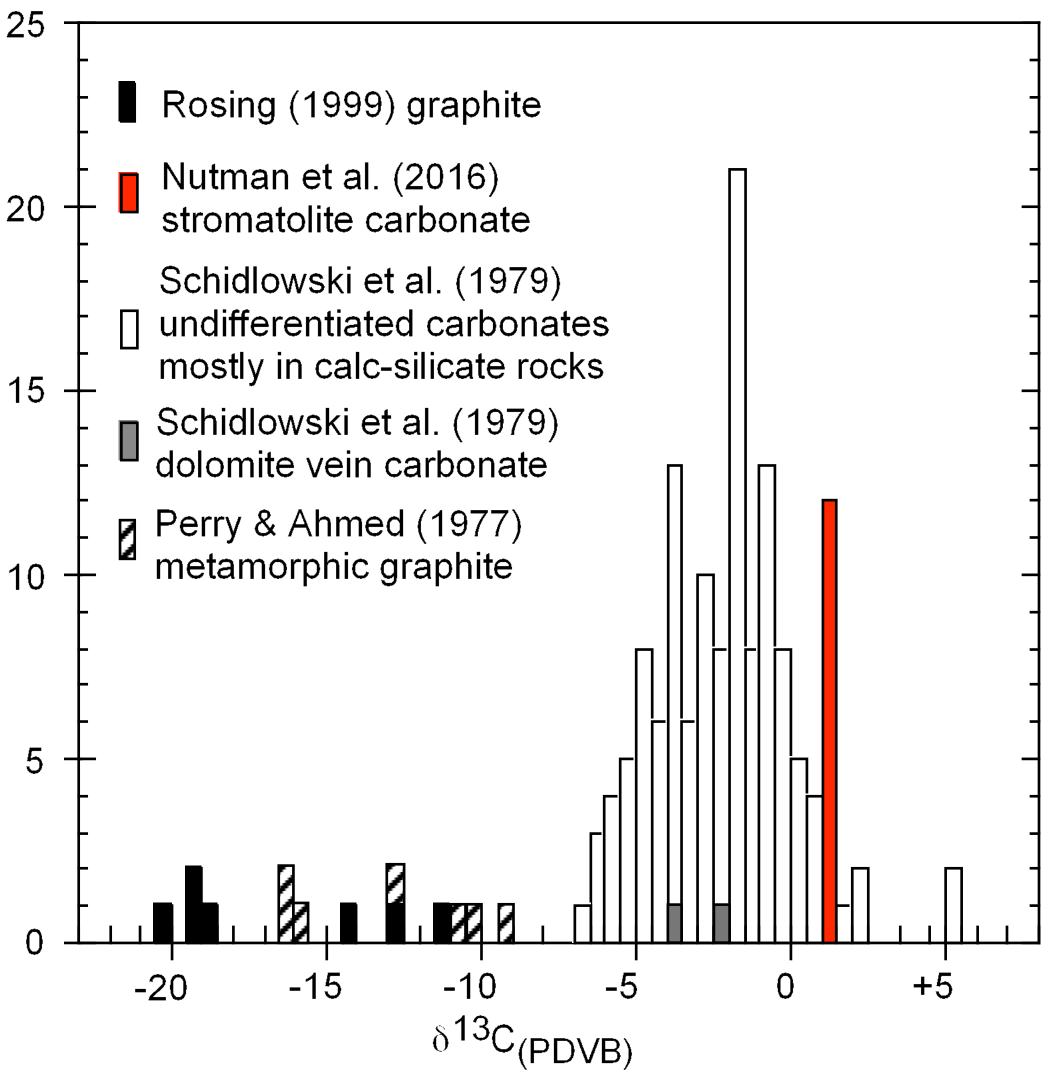
Rosing (1999) graphite
Nutman et al. (2016) stromatolite carbonate
Schidlowski et al. (1979) undifferentiated carbonates mostly in calc-silicate rocks
Schidlowski et al. (1979) dolomite vein carbonate
Perry & Ahmed (1977) metamorphic graphite
25
20
15
10
5
0
-20
-15
-10
-5
0
+5
$\delta^{13}C_{(PDVB)}$

sample ID	G11/63[a]	G11/72[a]	G05/54[b]	G05/55[b]	G91/75[b]	track[a]	track[a]	G11/71D (1)	G11/71D (2)	G11/71B (3)	G11/71B (4)	G17/32	G17/64
sample type	dolostone	clast rock	marble	marble	chert	strom A-9	dirty A-2	strom B	strom B	strom B	strom B	vein carb	vein carb
latitude (N)	65°10.153’	65°10.767’	65°10.820’	65°10.820’	65°12.092’	65°10.741’	65°10.741’	65°10.750’	65°10.750’	65°10.750’	65°10.750’	65°10.742’	65°07.016’
longitude (W)	49°49.479’	65°48.279’	49°48.283’	49°48.283’	49°47.688’	49°48.250’	49°48.250’	49°48.253’	49°48.253’	49°48.253’	49°48.253’	49°48.248’	50°13.220’
trace elements (p.p.m.)													
Si								0.6	0.5	0.2	1.1	0.68	0.1
P						85.9	8.2	13.9	9.1	11.5	11.9	25.5	21.4
Ti			391	34.3	11.5	116	1330	1.8	15.0	4.8	36.2	47.9	0.08
Cr	210	140	36.9	9	12.6	26	917	2.5	7.0	2.9	6.4	5.3	17.8
Ni			22.8	21	8.07	19.0	91.5	1.2	10.7	7.7	5.2	941	80.7
Rb	22.4	17	16.7	0.47	0.39	7.4	75.8	0.1	0.6	0.3	1.7	0.38	bld
Sr	63.4	17.5	18.1	9.83	1.61	34.8	29.5	99.8	39.5	51.7	79.2	4.16	562
Ba	1295	9640	349	5.00	1.00	886	3862	57	49	53	190	3.02	1.75
Y	6.6	8	3.15	2.38	0.85	4.51	10.8	22.5	2.48	6.77	15.3	7.58	76.6
Zr	9	14	13.5	1.99	0.52	5.2	28.9	12.7	15.0	1.7	4.3	bld	bld
Th	0.13	0.25	0.295	0.034	0.026	0.08	1.01	0.01	0.04	0.03	0.03	bld	bld
U	0.06	0.1	0.064	0.022	0.012	0.06	0.11	0.05	0.04	0.01	0.02	bld	bld
La	2.2	2.4	2.041	0.517	0.461	0.94	8.47	2.52	0.75	1.73	10.00	0.50	3.30
Ce	3.4	3.5	3.111	0.736	0.610	1.71	13.80	3.97	1.23	2.73	14.59	1.20	12.40
Pr	0.41	0.39	0.351	0.087	0.063	0.22	1.63	0.50	0.16	0.35	1.65	0.20	2.40
Nd	1.6	1.4	1.378	0.395	0.251	1.03	7.03	2.16	0.76	2.07	7.15	0.70	16.00
Sm	0.4	0.29	0.307	0.108	0.066	0.32	1.60	0.81	0.22	0.55	1.28	0.20	7.50
Eu	0.46	0.15	0.263	0.124	0.056	0.21	0.66	0.43	0.14	0.25	0.49	0.01	2.80
Gd	0.66	0.67	0.362	0.200	0.083	0.48	1.71	1.62	0.30	0.75	1.56	0.30	11.80
Tb	0.11	0.12	0.059	0.034	0.014	0.09	0.24	0.32	0.05	0.12	0.25	0.10	2.20
Dy	0.66	0.73	0.353	0.238	0.087	0.60	1.47	2.63	0.34	0.87	1.88	0.90	16.00
Ho	0.17	0.19	0.077	0.056	0.021	0.14	0.30	0.61	0.08	0.20	0.44	0.30	3.20
Er	0.46	0.53	0.230	0.174	0.059	0.41	0.87	2.08	0.22	0.63	1.44	1.40	9.80
Tm	0.07	0.08				0.06	0.13					0.30	1.50
Yb	0.46	0.49	0.211	0.150	0.060	0.39	0.89	2.03	0.21	0.65	1.46	1.90	7.80
Lu	0.09	0.08	0.033	0.023	0.008	0.07	0.12	0.32	0.03	0.10	0.22	0.30	1.20

a, Nutman et al. (2016); b, Friend et al. (2007)
Latitude and longitude with WGS84 datum